KAUNAS UNIVERSITY OF TECHNOLOGY

FACULTY OF MATHEMATICS AND NATURAL SCIENCES

Pranas Žiaukas

CHAOTIC PROCESSES AND THEIR APPLICATIONS IN COMPLEX DYNAMICAL SYSTEMS

Master's Degree Final Project

Supervisor
Prof. Dr. habil. Minvydas Ragulskis

KAUNAS, 2016

KAUNAS UNIVERSITY OF TECHNOLOGY

FACULTY OF MATHEMATICS AND NATURAL SCIENCES

CHAOTIC PROCESSES AND THEIR APPLICATIONS IN COMPLEX DYNAMICAL SYSTEMS

Master's Degree Final Project

M4026M21 Applied Mathematics (621G10003)

Supervisor

Prof. Dr. habil. Minvydas Ragulskis

2016 06 06

Reviewer

Prof. Dr. habil. Jonas Valantinas

2016 06 06

Project made by

Pranas Žiaukas

2016 06 06

KAUNAS, 2016

KAUNAS UNIVERSITY OF TECHNOLOGY

FACULTY OF MATHEMATICS AND NATURAL SCIENCES

Pranas Žiaukas

M4026M21 Applied Mathematics (621G10003)

”Chaotic processes and their applications in complex dynamical systems”

DECLARATION OF ACADEMIC INTEGRITY

6 June, 2016
Kaunas

I confirm that the final project of mine, Pranas Žiaukas, on the subject ”Chaotic processes and their applications in complex dynamical systems” is written completely by myself; all the provided data and research results are correct and have been obtained honestly. None of the parts of this thesis have been plagiarized from any printed, internet-based or otherwise recorded sources; all direct and indirect quotations from external resources are indicated in the list of references. No monetary funds (unless required by law) have been paid to anyone for any contribution to this thesis. I fully and completely understand that any discovery of any facts of dishonesty inevitably results in me incurring a penalty under procedure effective at Kaunas University of Technology.

Pranas Žiaukas

Žiaukas, Pranas. Chaotiniai procesai ir jų tyrimas sudėtingose sistemose. Magistro baigiamasis projektas / vadovas prof. habil. dr. Minvydas Ragulskis; Kauno technologijos universitetas, Matematikos ir gamtos mokslų fakultetas.

Mokslo kryptis ir sritis: fiziniai mokslai, matematika.

Reikšminiai žodžiai: dinaminės sistemos, chaosas, atraktoriai, fraktalinė dimensija, Wada savybė.

Kaunas, 2016. 50 p.

SANTRAUKA

Šiame darbe, panaudojant kelias skirtingas metodikas, atliekama chaotinių procesų analizė. Apibendrinta diskreti Niutono dinaminė sistema su kompleksiniu valdymo parametru modeliuojama kompiuterinėmis priemonėmis. Išgaunami skirtingi pritraukiančiųjų sričių išsidėstymo scenarijai, randamos šių sričių kraštų aibės. Kraštų fraktalinės dimensijos vertinamos naudojant ”dėžučių” skaičiavimo algoritmą. Pritraukiančiųjų sričių Wada savybės vertinamos naudojant naują pasiūlytą skaičiavimo algoritmą. Abi charakteristikos lyginamos parametrų plokštumoje, kurioje stebimos netrivialios jų tarpusavio sąsajos. Prie tam tikrų fiksuotų pradinių sąlygų pateikiami sudėtingo trajektorijų elgesio pavyzdžiai. Pabaigoje aptariami pasiūlytos Wada charakteristikos privalumai bei trūkumai, pateikiamos tolimesnių tyrimų rekomendacijos.

Žiaukas, Pranas. Chaotic processes and their applications in complex dynamical systems. Master's thesis in mathematics / supervisor prof. habil. dr. Minvydas Ragulskis. The Faculty of Mathematics and Natural Sciences, Kaunas University of Technology.

Research area and field: physical sciences, mathematics.

Key words: dynamical systems, chaos, attractors, fractal dimension, Wada property.

Kaunas, 2016. 50 p.

SUMMARY

Chaotic processes are analyzed in this thesis using multiple techniques. A relaxed Newton's discrete dynamical system with a complex control parameter is chosen and simulated numerically. Different set-ups of attracting basins are obtained along with their boundaries. The fractal dimensions of basin boundaries are measured using the box counting algorithm. The Wada qualities of basins are evaluated using a novel proposed algorithm. Both characteristics are compared in a two-dimensional parameter plane, non-trivial relations between them are emphasized. Examples of a complex transient behavior under certain conditions are provided. Finally, advantages and disadvantages of a proposed Wada characteristic are discussed, and recommendations are made regarding further research.

Contents

Introduction **8**

1 Overview **9**

1.1 Complex analysis . . . 9

1.1.1 Complex numbers . . . 9

1.1.2 Geometrical interpretation . . . 10

1.1.3 Differentiation . . . 11

1.1.4 Physical interpretation . . . 11

1.2 Discrete dynamical systems . . . 12

1.2.1 Introduction . . . 12

1.2.2 Attractors . . . 13

1.2.3 Chaotic properties . . . 14

1.2.4 Applications . . . 16

1.3 Fractals . . . 17

1.3.1 Concept . . . 17

1.3.2 Properties . . . 18

1.3.3 Numerical approximations . . . 19

1.3.4 Applications . . . 20

1.4 Motivation . . . 21

2 Methodology **22**

2.1 Newton's discrete dynamical system . . . 22

2.1.1 Introduction . . . 23

2.1.2 Properties . . . 24

2.1.3 Generalization . . . 25

2.1.4 Applications . . . 26

2.2 Fractal dimension . . . 26

2.2.1 Introduction . . . 26

2.2.2 Concept . . . 27

2.2.3 Algorithm . . . 29

2.2.4 Applications . . . 30

2.3 Wada measure . . . 30

2.3.1 Introduction . . . 30

2.3.2 Concept . . . 31
2.3.3 Algorithm . . . 32
2.3.4 Applications . . . 33

3 Research **34**
3.1 Analysis of basin boundaries . . . 34
3.1.1 Fractal dimension . . . 35
3.1.2 Wada measure . . . 37
3.1.3 Relation between characteristics . . . 39
3.2 Implications of chaos . . . 41
3.2.1 Uncertainty of the final attractor . . . 41
3.2.2 Controlling the dynamical system . . . 42
3.3 Discussion . . . 43

Conclusions **44**

Bibliography **45**

List of Figures

1.1 Geometrical interpretation of a complex number 10
1.2 Orbit of a dynamical system 12
1.3 Mandelbrot set 20

2.1 Basins of attraction for the Newton's discrete dynamical system 22
2.2 Basins of attraction for the NDDS with polynomials of higher order 23
2.3 H-ranks for the Newton's discrete dynamical system 24
2.4 Basins of attraction for the relaxed Newton's discrete dynamical system 25
2.5 Basin boundaries for the Newton's discrete dynamical system 28
2.6 The principle of box counting using boxes of various sizes ε. 29
2.7 Emergence of Wada property 31
2.8 The principle of Wada measure using boxes of various sizes ε. 33

3.1 Basins of attraction with very different values of fractal dimension. 35
3.2 Fractal dimensions for the relaxed NDDS with varying parameter $\alpha \in \mathbb{C}$. 35
3.3 Fractal dimension $D(\mathcal{F}_\alpha)$ in the parameter plane $\alpha \in \mathbb{C}$. 36
3.4 Basins of attraction with very different values of Wada measure. 37
3.5 Wada measures for the relaxed NDDS with varying parameter $\alpha \in \mathbb{C}$. 37
3.6 Wada measure $W(\mathcal{F}_\alpha)$ in the parameter plane $\alpha \in \mathbb{C}$. 38
3.7 Fractal dimensions $D(\mathcal{F})$ and Wada measures $W(\mathcal{F})$ for all parameters $\alpha \in \mathbb{C}_1$. . . 39
3.8 Minimum and maximum fractal dimensions for a fixed Wada measure 40
3.9 Uncertaintly of the final attractor 41
3.10 Trajectories of the NDDS orbits for the perturbed parameter $\alpha \in \mathbb{C}$ 42

Nomenclature

$\mathbb{C}$	Set of complex numbers
$\mathbb{C}_1$	Subset of complex numbers $[-1, 1]^2$
$\Re$	Real part of a complex number
$\Im$	Imaginary part of a complex number
Arg	Argument of a complex number
$\|.\|$	Modulus of a complex number
$\mathbb{N}$	Set of natural numbers
$\mathbb{R}$	Set of real numbers
RMSE	Root mean square error
$z_{n+1} = f(z_n)$	Discrete nonlinear map
$\mathbb{Z}$	Set of integers
$f^{\circ n}$	Superposition of f applied n times
$\mathcal{A}$	Set of attracting points
$\mathcal{N}$	Set of neighboring points
$\mathcal{B}$	Basin of attraction
λ	Lyapunov exponent
log	Natural logarithm
M_k	Hankel matrix of order k
det	Determinant
H	Hankel rank
$\mathcal{F}$	Fractal set
IFS	System of iterated functions
$\mathcal{H}$	Collection of non-empty compact sets
d	Metric function
ω	Conformal transformation
F	Fatou set
J	Julia set
NDDS	Newton's discrete dynamical system
p	Polynomial function
D	Fractal dimension
W	Wada measure
ρ	Pearson's correlation coefficient
r	Spearman's correlation coefficient

Introduction

Attractors are some of the most important sets in the theory of nonlinear dynamical systems. Analysis of attractors along with their basins of attraction is crucial in order to understand the behavior of a given dynamical relation. This knowledge can be applied with the purpose to simulate and control a particular system, measure the associated uncertainty, or in various other cases. As contemporary researchers seek to improve the state-of-the-art algorithms, novel methods are proposed in the field of nonlinear dynamics on a regular basis [1].

An example of a relatively simple system which possesses some rich chaotic dynamics is

$$f_p(z) = z - \alpha \frac{p(z)}{p'(z)};$$

where argument $z \in \mathbb{C}$, parameter $\alpha \in \mathbb{C}$, and p is a complex-valued polynomial function. This is known as a Newton's method [2]. Despite the apparent simplicity, its boundaries of attracting basins are not simple smooth curves but rather fractal shapes [3]. Moreover, sometimes these basins of attraction are interwoven infinitely many times, which is also known as a Wada quality [4].

The general aim of this thesis is to develop and propose some novel tools and techniques for the analysis of chaotic processes in complex dynamical systems.

The aim is achieved by accomplishing the following tasks:

1. Generate a large family of different set-ups of attracting basins.
2. Calculate the complexity of boundaries using known techniques.
3. Re-calculate the complexity of boundaries using novel proposed tools.
4. Compare the obtained results regarding complexity.
5. Provide relevant examples of applications.

Overview

In a relatively short and concise overview the necessary theoretical preliminaries and widely accepted concepts used in this work are described.

Section 1.1 is dedicated to the realm of complex numbers and complex analysis, section 1.2 introduces discrete dynamical systems and, lastly, section 1.3 presents some general ideas regarding self-similarity and fractals.

1.1. Complex analysis

Initially, some real numbers $x, y \in \mathbb{R}$ are considered. Under the well-known operations of addition "$+$", subtraction "$-$", multiplication "$\cdot$" or division "$\div$" the resulting quantities remain real. However, in case of square roots (such as $\sqrt{x}$), or solutions to polynomial equations with real coefficients (such as $x^2 = -1$) the property of being real does not hold anymore. It has been accepted that sometimes there are no solutions to the proposed problems amongst real numbers $\mathbb{R}$ (see [5]). An alternative is to use a more general realm - like the set of complex numbers $\mathbb{C}$.

1.1.1. Complex numbers

The earliest references to the concept of complex numbers are attributed to the mathematicians of the ancient Greece [6]. The notion of an imaginary unit $\sqrt{-1}$ was introduced in the sixteenth century, and later became (as discussed in [7]) simplified as i. Over years the idea matured and evolved into the modern notion of complex numbers that is known nowadays.

Definition 1.1. A **complex number** is a pair $z = x + iy$, where the components $x, y \in \mathbb{R}$ and i is an imaginary unit satisfying $i^2 = -1$. The set of all complex numbers is denoted $\mathbb{C}$. □

Following the introduced notation, for any complex number $z = x + iy \in \mathbb{C}$ there is two parts:

- **real part** $\Re(z) = x$, that does not have an imaginary unit;
- **imaginary part** $\Im(z) = y$, that, on the contrary, is matched with an imaginary unit.

All the arithmetical operations are accomplished in an intuitive way, as in $\mathbb{R}$. Real and imaginary parts are treated as separate summands.

Example 1.1. The multiplication of two complex numbers z_1 and z_2 is accomplished as follows

$$z_1 \cdot z_2 = (x_1 + iy_1) \cdot (x_2 + iy_2) = x_1x_2 + ix_1y_2 + iy_1x_2 + i^2y_1y_2 = \\ = x_1x_2 + ix_1y_2 + iy_1x_2 - y_1y_2 = (x_1x_2 - y_1y_2) + i(x_1y_2 + y_1x_2).$$

1.1.2. Geometrical interpretation of complex numbers

Typically real and imaginary parts (say x and y) of a given complex number $z \in \mathbb{C}$ are interpreted as components of some vector $(x, y) \in \mathbb{R}^2$ in a Euclidean plane. It is a consequence of the fact that there exists a bijective mapping between $\mathbb{C}$ and $\mathbb{R}^2$. In other words, every complex number z may be assigned a vector (x, y) as its visual counterpart, and vice versa. It is known as a geometrical representation of a given complex number [6]. The idea is illustrated in figure 1.1.

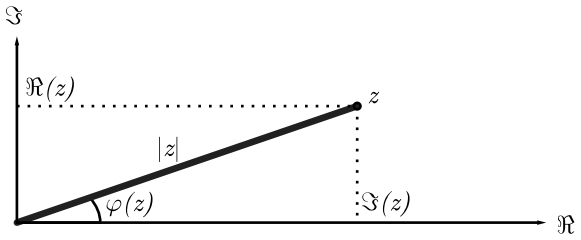

Figure 1.1: Geometrical interpretation of a complex number. This includes real and imaginary parts $\Re(z)$ and $\Im(z)$ respectively, complex modulus $|z|$, and also argument $\varphi(z)$.

In terms of classical geometry, a two-dimensional vector may be characterized by its length, angle with respect to some axis, and other properties. Since there exists a direct correspondence between Euclidean $\mathbb{R}^2$ and complex $\mathbb{C}$ planes, the very same idea applies to complex numbers. Therefore some more relevant definitions regarding complex numbers are presented below.

Definition 1.2. The **modulus** (or the **norm**) of a complex number $z = x + iy$ is denoted and defined as $|z| = \sqrt{x^2 + y^2}$. □

It should be added that generally norm is a function that maps vectors to positive numbers (except the origin vector which is mapped to zero) and satisfies the properties of scalability, sub-additivity and separability [8]. Thus there can be different norms that are equally acceptable in a particular field of mathematics. However, in this work the classical context is used, and the traditional case of complex modulus is presented.

Definition 1.3. The **argument** of a complex number $z = x + iy$ is the angle $\varphi \in [0; 2\pi)$ between the vector (x, y) and the real positive semi-axis $\mathbb{R}^+$. It is denoted $\mathrm{Arg}(z)$. □

Once again, there are different interpretations of this characteristic. For example, the values of an angle φ can be chosen from $[-\pi; \pi)$ or, for the sake or argument, even $[-2\pi; 0)$. This would not go against mathematical requirements. In this work the interval $[0; 2\pi)$ is selected.

1.1.3. Differentiation of complex functions

In case of real numbers, the idea of differentiation arises from the need to compute instantaneous velocities or slopes of tangent lines. In case of complex numbers, the differentiation is not so intuitive. However, in both cases it is a matter of computing some limit values.

Definition 1.4. Function $f(z)$ is **differentiable** at a point $z_0 \in \mathbb{C}$ if it is defined in the neighborhood of z_0 and the following limit exists

$$f'(z_0) = \lim_{z \to z_0} \frac{f(z) - f(z_0)}{z - z_0}. \tag{1.1}$$

$f'(z_0)$ is then referred to as the **derivative** of f at z_0. □

One important aspect that is not present in the case of real numbers, is that the limit value has to be approached from infinitely many directions instead of just two. Furthermore, it is not a straightforward procedure to interpret or visualize the outcome when the function f is of complex nature. In some cases, it can be really challenging or even impossible [9].

Example 1.2. Let's compute the derivative of $f(z) = z^3$ for all $z \in \mathbb{C}$,

$$f'(z) = \lim_{\Delta z \to 0} \frac{(z + \Delta z)^3 - z^3}{\Delta z} = \lim_{\Delta z \to 0} \frac{z^3 + 3z^2\Delta z + 3z\Delta z^2 + \Delta z^3 - z^3}{\Delta z} =$$
$$= \lim_{\Delta z \to 0} \frac{3z^2\Delta z + 3z\Delta z^2 + \Delta z^3}{\Delta z} = \lim_{\Delta z \to 0} \left(3z^2 + 3z\Delta z + \Delta z^2\right) = 3z^2.$$

1.1.4. Physical interpretation of complexity

The complex derivative cannot be interpreted as an instantaneous velocity or some steepness of a tangent slope. No quantities can be measured nor counted as imaginary values in a usual tangible sense. Despite all that, complex numbers are quite useful for enhancing different types of mathematics, generalizing ideas, and extending the scope of real numbers [7].

- The complex modulus is directly related to the notions of magnitude, distance, and absolute value in various physical contexts.
- The argument represents rotational characteristics and positioning in space.
- The existence of complex derivative is a very strong condition which comes in pair with an opposite effect of integration.

As a consequence, in fluid dynamics complex valued functions are used to describe potential flows [10]. Closely related disciplines such as aerodynamics, hydrodynamics, and hydraulics have a range of applications that require usage of two dimensional quantities as well [11]. In electrical engineering, the characteristics of resistors, capacitors, and inductors can be combined by introducing imaginary resistances [12]. In special and general relativity, some formulas manipulate complex values, including the famous Schrödinger equation in quantum mechanics [13].

All this is part of the foundation of modern mathematics and mathematical physics that would not be possible without complex analysis.

1.2. Discrete dynamical systems

During recent decades the discipline of nonlinear dynamics has grown significantly [14]. Introduction of deterministic chaos and nonlinearity have provided some new and innovative tools that allow scientific community to better assess and understand surprisingly complex behaviors of relatively simple systems. The aim of this subsection is to provide some preliminaries that are necessary in order to proceed with the complete research of this work.

1.2.1. Introduction to discrete dynamical systems

In case of discrete-time dynamical systems, the dynamics are fully described by some iterated maps, also known as evolutionary functions [15].

Definition 1.5. An **iteration** of a discrete dynamical system is a function f of the form

$$z_{n+1} = f(z_n); \tag{1.2}$$

that takes and returns complex values $z_n, z_{n+1} \in \mathbb{C}$. □

It is understandable that some further restrictions may be enforced on argument z_n. The model may only be valid under certain circumstances or in specific situations. However, these restrictions vary from system to system.

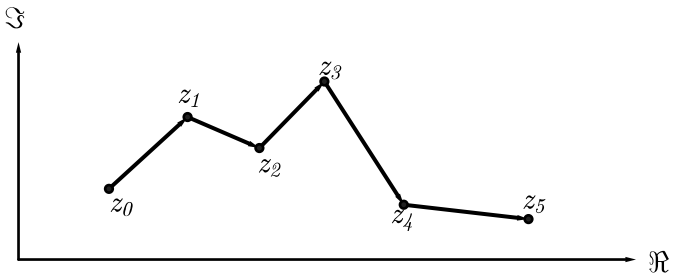

Figure 1.2: Orbit of a given dynamical system. Initial seed z_0 evolves into $f(z_0) = z_1$, then $f(z_1) = z_2$ and so on as required.

Another important notion is to realize that the evolution of z_0 may be immensely complex as the iterations proceed in time under the specified rule f.

Definition 1.6. For a given dynamical system f, the **orbit** of $z_0 \in \mathbb{C}$ is the sequence of iterates

$$(z_0,\ z_1,\ z_2,\ \ldots) = \Big(z_0 \quad f(z_0) \quad f(f(z_0)) \quad \ldots\Big); \tag{1.3}$$

also referred to as a trajectory of z_0. □

It is typical to denote the repeated applications of f using the notation of superposition

$$f^{\circ n}(z_0) = \underbrace{f(f(\ldots f(}_{n \text{ times}} z_0)\ldots). \tag{1.4}$$

One of the main objectives in the modern theory of dynamical systems is to fully understand the properties of orbits (see figure 1.2) [16].

Example 1.3. Let's look at the specific orbit of the discrete dynamical system described by the map $f(z) = 3z(1-z)$. An initial seed $z_0 = 1/3$ is fixed and further investigated

$$\begin{aligned}
&z_0 = 1/3,\\
&z_1 = f(z_0) = f(1/3) = 3 \cdot 1/3 \cdot (1 - 1/3) = 2/3,\\
&z_2 = f(z_1) = f(2/3) = 3 \cdot 2/3 \cdot (1 - 2/3) = 2/3, \quad \text{and generally}\\
&z_n = f(z_{n-1}) = 2/3, \quad \text{whenever } n \in \mathbb{N}.
\end{aligned}$$

A precise orbit $(1/3,\ 2/3,\ 2/3,\ \ldots)$ which converges relatively quickly is obtained. The topics of attractors and convergence are discussed in the following subsections.

1.2.2. Attractors of discrete dynamical systems

Dynamical systems may possess one or several attractors. Simply put, attractors are structures which initial conditions tend to evolve to. Some more rigorous definitions are presented in [1, 16, 17]. One of possible approaches is formulated in this subsection.

Definition 1.7. An **attractor** is a set of points $\mathcal{A} \subset \mathbb{C}$ that is invariant under the dynamics, that is

$$\forall z_0 \in \mathcal{A} \quad z_1 = f(z_0) \Rightarrow z_1 \in \mathcal{A}; \tag{1.5}$$

and towards which some neighborhood $\mathcal{N} \subset \mathbb{C}$ evolutes in the course of time

$$\forall z_0 \in \mathcal{N} \quad z_n = f(z_{n-1}) \Rightarrow \lim_{n \to +\infty} z_n \in \mathcal{A}. \tag{1.6}$$

It is also the smallest unit which cannot be divided into two or more attractors with distinct neighborhoods $\mathcal{N}$. □

Additionally, an attractor satisfies the following conditions:

1. $\mathcal{A}$ is a bounded and closed set that is invariant under the dynamical system.
2. $\mathcal{A}$ attracts some open neighborhood of initial conditions.
3. $\mathcal{A}$ is strictly minimal and has no proper subset satisfying previous conditions.
4. $\mathcal{A}$ is stable in terms of Lyapunov stability.
   In simple terms, if the solutions around an attractor $\mathcal{A}$ stay in that vicinity forever, then $\mathcal{A}$ is Lyapunov stable.

An attractive set $\mathcal{A}$ has some peculiar properties. Once the attracting neighborhood $\mathcal{N}$ is determined, it follows that the distance from an arbitrary element $z_0 \in \mathcal{N}$ to $\mathcal{A}$ (in terms of a Euclidean metric) tends to diminish over time. This is a crucial concept. The largest such set is known as the basin of attraction.

Definition 1.8. The largest set $\mathcal{N} \subset \mathbb{C}$ such that its members approach $\mathcal{A}$ over time

$$\forall z_0 \in \mathcal{N} \quad \lim_{n \to +\infty} d(z_n, \mathcal{A}) = 0; \tag{1.7}$$

is called the **basin of attraction** $\mathcal{B}(\mathcal{A})$ or simply $\mathcal{B}$. □

It is quite common for discrete dynamical systems to have multiple attractors [15]. For each such attractor, there exists a corresponding basin of attraction which consists of distinct elements taken from the complex plane $\mathbb{C}$.

Example 1.4. Let's look at the attractors of the discrete dynamical system described by the map $f(z) = z/2$. For an arbitrary initial seed $z_0 \in \mathbb{C}$, it is evident that

$$\lim_{n \to +\infty} f^{\circ n}(z_0) = \lim_{n \to +\infty} (z_0/2^n) = 0.$$

By definition, it can be concluded that the system has a single attractor $\mathcal{A} = \{\, 0 \,\}$ with its basin of attraction being the whole complex plane $\mathcal{B} = \mathbb{C}$.

1.2.3. Chaotic properties of discrete dynamical systems

There are many different met hods to look at the chaotic properties of a given dynamical system [18]. One of the signs of chaos is the rapid divergence of nearby trajectories. In fact, this divergence is sometimes even exponential in time (or with respect to iterations). Similarly, there are various different tools proposed to effectively analyze chaos. These, for example, are Lyapunov exponents or H-ranks that are presented in this subsection.

Lyapunov exponents

Say that an initial seed belongs to some attractor $z_0 \in \mathcal{A}$. Let's look at how z_0 differs from $z_0 + \varepsilon$ over time for some arbitrary difference $\varepsilon \in \mathbb{C}$. In other words, an iterated map f is applied. Then the absolute difference between the orbits (previously defined as complex modulus 1.2) is

$$d_n = |f^{\circ n}(z_0 + \varepsilon) - f^{\circ n}(z_0)|. \tag{1.8}$$

In case that the behavior is chaotic, then the divergence should be exponential on n

$$\frac{d_n}{\varepsilon} = \frac{|f^{\circ n}(z_0 + \varepsilon) - f^{\circ n}(z_0)|}{\varepsilon} = e^{\lambda n}. \tag{1.9}$$

After expressing power λ, the result is

$$\lambda = \frac{1}{n} \log \left(\frac{|f^{\circ n}(z_0 + \varepsilon) - f^{\circ n}(z_0)|}{\varepsilon} \right). \tag{1.10}$$

This defines what is meant by the speed of divergence. When $\varepsilon \to 0$ and the chain rule for differentiation is applied, then the strict definition of Lyapunov exponent is obtained.

Definition 1.9. The **Lyapunov exponent** around $z_0 \in \mathbb{C}$ is defined by

$$\lambda = \frac{1}{n} \log \left(\prod_{k=0}^{n-1} |f'(z_k)| \right) = \frac{1}{n} \sum_{k=0}^{n-1} \log \left(|f'(z_k)| \right). \tag{1.11}$$

It is the rate of divergence between two neighboring trajectories. □

In the presented definition the Lyapunov exponent is calculated only at a single point $z_0 \in \mathbb{C}$. However, in the literature [19] it is usual to define the average Lyapunov exponent over all valid initial seeds. Then it is said that a given discrete dynamical system has chaotic trajectories if the average Lyapunov exponent is positive [20].

H-ranks

Begin by establishing a structural matrix whose elements depend only on the sum of their indices. It is known as a Hankel matrix [21].

Definition 1.10. A **Hankel matrix** of depth $k \in \mathbb{N}$ (also known as a catalecticant, persymmetric matrix [22]), is a square matrix

$$M_k = \begin{pmatrix} z_0 & z_1 & \dots & z_{k-1} \\ z_1 & z_2 & \dots & z_k \\ \vdots & \vdots & \ddots & \vdots \\ z_{k-1} & z_k & \dots & z_{2k-2} \end{pmatrix}; \tag{1.12}$$

whose skew-diagonal elements from left to right are constant. □

An orbit $(z_0,\ z_1,\ z_2,\ \ldots)$ of some dynamical system can be used to populate the Hankel matrix. The so-called Hankel transform of this orbit yields a sequence of determinants $\det(M_k)$.

Definition 1.11. The orbit $(z_0,\ z_1,\ z_2,\ \ldots)$ is of n-th order if

$$\det(M_n) \neq 0, \qquad \det(M_{n+k}) = 0,\ \forall k \in \mathbb{N}. \tag{1.13}$$

This integer value is known as H**-rank** and noted $H(z_0,\ z_1,\ z_2,\ \ldots) = n$. □

Hankel rank is an important tool in evaluation of convergence rates, especially in discrete chaotic maps. The higher the rank, the more complex the calculated trajectory. The rate of convergence analyzed on a wide scale may provide some insights into the nature of some dynamical attractors [23].

Example 1.5. Let's check the H-rank of a simple sequence $(e,\ \pi,\ e, \pi,\ \ldots)$ where odd-positioned elements are equal to e and even-positioned elements are equal to π. Proceed by taking some Hankel matrices and their corresponding determinants

$$\det(M_1) = \det(e) = e \neq 0;$$
$$\det(M_2) = \det \begin{pmatrix} e & \pi \\ \pi & e \end{pmatrix} = e^2 - \pi^2 \neq 0;$$

which happen to be non-zero. The tendency can be noticed

$$\det(M_3) = \det \begin{pmatrix} e & \pi & e \\ \pi & e & \pi \\ e & \pi & e \end{pmatrix} = 0;$$
$$\det(M_4) = \det \begin{pmatrix} e & \pi & e & \pi \\ \pi & e & \pi & e \\ e & \pi & e & \pi \\ \pi & e & \pi & e \end{pmatrix} = 0;$$

and similarly $\det(M_k) = 0$ for all $k > 2$ because odd-positioned rows of the Hankel matrices are the same as the even-positioned rows. Then by definition $H(e,\ \pi,\ e, \pi,\ \ldots) = 2$. It means that the complexity of the sequence in question is of order two. This fact is understandable because there are precisely two alternating elements in the sequence.

1.2.4. Applications of dynamical systems

There are applications of nonlinear dynamical systems in virtually every field of science.

In the field of medicine and chemistry, applications include genetic control systems [24], biological rhythms of various neuronal systems [25], search of cure for cancer or other highly complex diseases [26].

In biology, insect outbreaks are modeled and predicted [27] alongside with management and analysis of animal populations in general [28].

Contemporary engineering includes studies of superconducting circuits and quantum simulations [29], building sophisticated oscillators in meta-materials [30], measuring mechanical vibrations [31, 32] with extreme precision.

Computer science revolves around improving algorithms of optimization with meta-heuristic approaches to solve structural problems [33], multi-label machine learning and classification [34] and even techniques for using chaos to send encrypted messages [35].

In each and every case, the scientific background varies but is generally closely integrated with the mathematical theory.

1.3. Fractals

Many physical systems in nature and many artifacts in human activities are not actually regular geometric shapes. These shapes do not conform to the standard geometry derived by Euclid. Aforementioned shapes belong to some more general geometry which offers more ways of describing, measuring and predicting natural phenomena. It is known as a fractal geometry [36].

1.3.1. The concept of fractality

In spite of some common sense concepts of fractals, it is not that easy to give a rigorous definition for one. According to Mandelbrot [37], it is "a rough or fragmented geometric shape that can be split into parts, each of which is (at least approximately) a reduced-size copy of the whole". Sometimes a strict definition for an arbitrary fractal structure is given by the following definition.

Definition 1.12. A set or structure $\mathcal{F}$ whose Hausdorff-Besicovitch dimension (see section 2.2) strictly exceeds its topological dimension is called a **fractal**. □

The above definition, no matter how precise, is quite difficult to apply in practice because the Hausdorff-Besicovitch characteristic itself possesses quite a complicated nature. As a matter of fact, for a lot of widely used fractals it is the case that the exact Hausdorff-Besicovitch dimension is unknown. Therefore, some alternative and usually easier to evaluate definitions of fractal structures are used along with some compromises.

Besides, there exist different types of fractals. Two of the most prevalent types are: Iterated function system (IFS) fractals and algebraic fractals.

Iterated function system fractals

Iterated function system fractals are obtained by using transformations in a space $(\mathcal{H}, d)$ of non-empty compact sets $\mathcal{H}$ (possibly subsets of $\mathbb{R}^2$) and some metric $d\colon \mathcal{H}^2 \to \mathbb{R}^+$. Transformations are conformal and include scaling, translation and rotation [38].

The creation of an iterated function system IFS fractal consists of defining a set of multiple conformal transformations $\{\, \omega_k\colon \mathcal{H} \to \mathcal{H} \mid k = \overline{1, \ldots, n} \,\}$ and finding its fixed point $\mathcal{F} \in \mathcal{H}$ under the set union operation W

$$\mathcal{F} = W(\mathcal{F}) = \bigcup_{k=1}^{n} w_k(\mathcal{F}). \tag{1.14}$$

This fixed point $\mathcal{F}$ is the fractal of interest. Some of the most famous IFS fractals are the Sierpinski triangle and the Koch snowflake [39].

Algebraic fractals

Fractals may be created by applying a discrete dynamical system $f\colon \mathbb{C} \to \mathbb{C}$ repeatedly. Since the iteration $f(z_k) = z_{k+1}$ must be applied indefinitely many times, computational techniques are almost always necessary in order to generate, investigate and see the visual representation of the

fractal [40]. Concepts of Julia set J and Fatou sets F_k are used to describe two complementary sets obtained from an evolutionary function f [41].

The Fatou set F_k, for some $k \in \mathbb{N}$, of the function f consists of elements with the property that all nearby values behave similarly under the repeated iteration of the function, for example converge to some attractor $\mathcal{A}_k$. It is also completely invariant under iterations, meaning

$$f^{-1}(F_k) = f(F_k) = F_k. \tag{1.15}$$

On the contrary, the Julia set J consists of values such that an arbitrarily small perturbation can cause drastic changes in the sequence of iterated function values. No convergence may be predicted. It is the complement of all aforementioned Fatou sets

$$J = \mathbb{C} \setminus \bigcup_k F_k. \tag{1.16}$$

In this case the Julia set is the fractal entity of interest $J = \mathcal{F}$.

Example 1.6. Let's investigate a particular complex-valued function $f(z) = z^2$, $z \in \mathbb{C}$. According to the discussed properties of complex numbers (see section 1.1), it is understandable that

$$\forall z \in \mathbb{C} \quad |z| < 1 \Rightarrow \lim_{n \to +\infty} f^{\circ n}(z) = \lim_{n \to +\infty} |z|^n e^{in \operatorname{Arg}(z)} = 0.$$

So the values inside a unit circle converge to a particular attractor $\mathcal{A}_1 = \{\, 0 \,\}$. Moreover, they form a Fatou set $F_1 = \{\, z \in \mathbb{C} \mid |z| < 1 \,\}$. Similarly, there is an effect

$$\forall z \in \mathbb{C} \quad |z| > 1 \Rightarrow \lim_{n \to +\infty} f^{\circ n}(z) = \lim_{n \to +\infty} |z|^n e^{in \operatorname{Arg}(z)} = +\infty;$$

which makes sense only in an extended complex plane. Simply put, all the values diverge in a similar manner and therefore form a second Fatou set $F_2 = \{\, z \in \mathbb{C} \mid |z| > 1 \,\}$.

The complement $J = \mathbb{C} \setminus (F_1 \cup F2) = \{\, z \in \mathbb{C} \mid |z| = 1 \,\}$ is a Julia set. When the function f acts upon the values of a Julia set, then the angles are doubled $\operatorname{Arg}(f(z)) = 2 \operatorname{Arg}(z)$ for $z \in J$. The operation is also chaotic for the points where complex argument is not a fraction of 2π.

1.3.2. Properties of fractals

Two of the most apparent properties of fractals are self-similarity and non-integer dimension. Despite the disagreements on the exact definition, authors usually emphasize at least the basic ideas of self-similarity and an unconventional relationship with the space a fractal is embedded in.

According to widespread research [42] here are some of the characteristics used to describe fractal structures. In other words, a set $\mathcal{F}$ that has the property of fractality tends to satisfy the following conditions more often than not:

1. $\mathcal{F}$ has a detailed and fine structure on arbitrary small scales.

2. $\mathcal{F}$ is locally and globally irregular in terms of Euclidean geometry.

3. $\mathcal{F}$ possesses a property of self-similarity.

4. $\mathcal{F}$ has some fractal dimension which is greater than its topological dimension.

5. $\mathcal{F}$ can be defined with ease using recursive or iterative methods.

1.3.3. Numerical approximations of fractals

The deterministic algorithm

For a set of multiple conformal transformations $\{\, \omega_k \colon \mathcal{H} \to \mathcal{H} \mid k = \overline{1, \ldots, n} \,\}$ it is possible to approximate the corresponding IFS fractal using (**1.14**)

$$\mathcal{F} = \bigcup_{k=1}^{n} w_k(\mathcal{F}). \tag{1.17}$$

Initially an arbitrary compact set $A_0 \in \mathcal{H}$ is chosen. Then a sequence of successive elements $A_k = W(A_{k-1})$, $k \in \mathbb{N}$, is computed, that is $(A_0,\ A_1,\ A_2,\ \ldots, A_n)$. By theorem of contractive mappings (the proof can be found in [43]), this sequence converges to the fixed point of the IFS

$$\lim_{n \to +\infty} A_n = \mathcal{F}. \tag{1.18}$$

If a finite, yet sufficiently large, timespan $n \in \mathbb{N}$ is chosen, then the resulting set A_n is an approximation of $\mathcal{F}$.

The random iteration algorithm

Once again let's start off with a set of multiple conformal transformations $\{\, \omega_k \colon \mathcal{H} \to \mathcal{H} \mid k = \overline{1, \ldots, n} \,\}$. This time a probability $p_k > 0$ is assigned to each transformation ω_k and additionally $\sum_{k=1}^{n} p_k = 1$. The probabilities are typically based on the coefficients of contractivity that certain transformations possess.

Initially an arbitrary point z_0 is chosen from any element of $\mathcal{H}$, so typically $z_0 \in \mathbb{C}$ or $z_0 \in \mathbb{R}^2$. Then during every iteration, a next point z_t, $t \in \mathbb{N}$, is chosen recursively and independently

$$z_t \in \{\, \omega_1(z_{t-1}), \omega_2(z_{t-1}), \ldots, \omega_n(z_{t-1}) \,\}; \tag{1.19}$$

with the probability of an event $z_t = \omega_k(z_{t-1})$ being p_k. A resulting collection of such points $\{\, x_t \mid t \in \mathbb{N} \,\}$ approximates the fractal $\mathcal{F}$. The proof of this fact can be found in [43].

The escape time algorithm

This algorithm compares how fast an arbitrary point $z_0 \in \mathbb{C}$ escapes a given boundary under the action of some dynamical system $f \colon \mathbb{C} \to \mathbb{C}$. Intuitively, it is expected that some orbits of the dynamical system settle to some attractor $\mathcal{A}_k$ slower than others. For example, initial seeds that are close to the boundary of corresponding Fatou sets F_k, for some $k \in \mathbb{N}$, may demonstrate a complicated behavior [44].

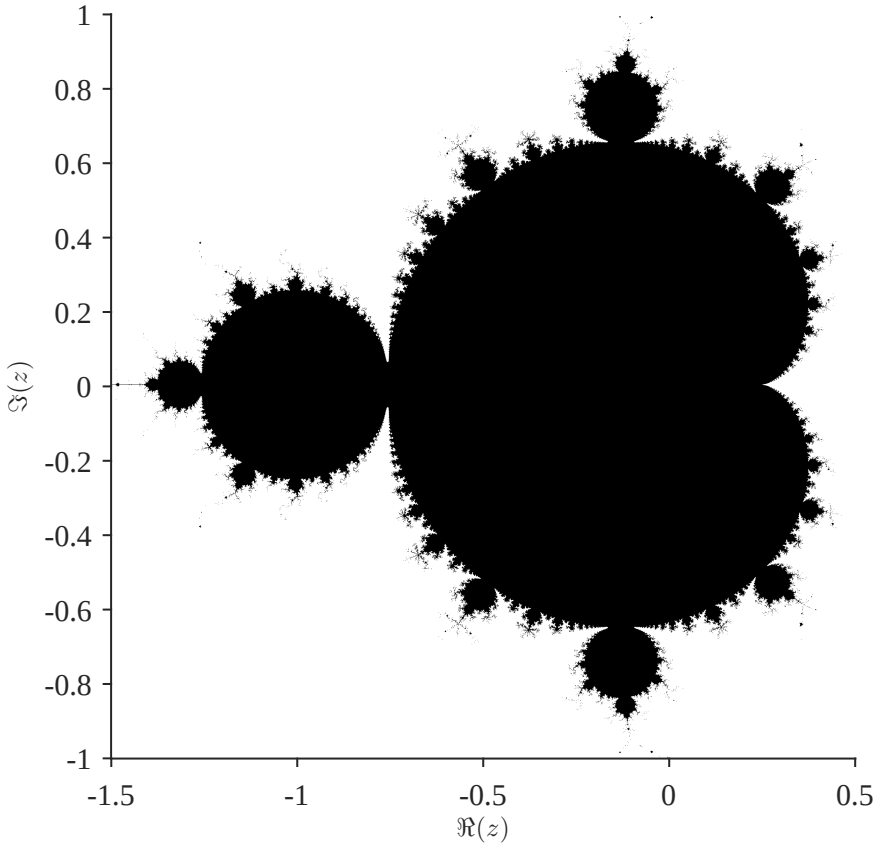

Figure 1.3: Approximation of the Mandelbrot set. Selected points (color black) do not escape the boundary circle $|z| = 2$ after $n = 50$ iterations.

In fact, it can be the case that some points never converge to any of the attractors. They are precisely the points of Julia set J and the fractal $\mathcal{F}$ which is the subject of interest. During the algorithm, it is investigated whether a finite orbit $(z_0, z_1, \ldots, z_n)$ crosses some boundary around the attracting set $\mathcal{A}$. The decision is made based on the following facts:

1. If the boundary is crossed at or before the time $n \in \mathbb{N}$, then $z_0 \notin \mathcal{F}$.

2. If the whole finite orbit $(z_0, z_1, \ldots, z_n)$ stays inside the boundary, then $z_0 \in \mathcal{F}$.

Example 1.7. Consider a Mandelbrot set. By definition this set consists of complex numbers $c \in \mathbb{C}$ for which the discrete dynamical system $f(z_k) = z_k^2 + c$, $k \in \mathbb{N}$, does not diverge when iterated from a constant initial seed $z_0 = 0$.

Choose a complex boundary circle $|z| = 2$ and state that the system diverges if this boundary is crossed (this fact is proved in [37]). Then investigate different values $c \in \mathbb{C}$ for the orbits of length $n = 50$. The visual result is presented in figure 1.3. The parameters $c \in \mathbb{C}$ that do not cause the suspected divergence are painted black. This is an approximation of the Mandelbrot set.

1.3.4. Applications of fractals

Fractal geometry has influenced many areas of contemporary science such as biology, astrophysics, engineering and especially techniques in computer graphics.

Fractals appear in biological sciences as representations of animal movement [45] and the structure of their habitat [46]. Additionally, the basic architecture of a chromosome is believed to be fractal-like [47] similarly to the DNA sequences [48].

In astrophysics, the formation process of interstellar clouds is believed to resemble a formation process of fractals [49]. The universe appears as if it is a classically self-similar random process at all astrophysical scales [50]. Galaxy samples are considered to possess fractal properties [51].

There are applications of fractals in the field of engineering. In antennas, the fractal shapes are translated into the electromagnetic behavior [52]. Self-similar processes and multifractal processes are needed in order to model a network traffic [53]. The growth or urban ares can be described using fractal techniques [54].

Finally, fractals are used in computer science. Image compression schemes use fractal algorithms to compress graphic files [55]. Artists use self-similar forms to create, model and present textured landscapes, mountain ranges and coastlines [56]. Fractal art and architecture is believed to possess an aesthetic quality based on their visual complexity [57].

Overall, fractal concepts can be used to model natural objects. They allow to mathematically define the used environment with high accuracy and precision.

1.4. Motivation of thesis

In order to accomplish the aims of this thesis, it is adequate to choose a family of complex discrete dynamical systems. The set of complex numbers $\mathbb{C}$ is a substantial generalization over a set of real numbers $\mathbb{R}$. Consequently, more advanced tools can be adopted and more profound insights can be made if a complex-valued function f is chosen.

The aforementioned systems are to be thoroughly evaluated in terms of complexity and transient dynamics. Discrete dynamical systems $z_{n+1} = f(z_n)$, where $n \in \mathbb{N}$, may exhibit highly non-trivial behavior that is not initially apparent. Advanced techniques are required to describe and measure the chaotic tendencies.

Attracting basins and their boundaries are to be evaluated in terms of fractal geometry. Fractals $\mathcal{F}$ are the results of chaos. These sets may form structures that are fully connected yet discontinuous everywhere, and have non-integer dimensions.

Finally, numerical results are to be compared and conclusions are to be made.

Methodology

The purpose of a more detailed methodology is to present the ideas and algorithms that are originally applied in this work.

Section 2.1 is dedicated to the discrete Newtonian dynamical system and its generalizations. Section 2.2 introduces box counting algorithm which is used to evaluate the fractal dimension of a basin boundary. Lastly, section 2.3 presents a novel algorithm for measuring Wada property of some basins of attraction.

2.1. Newton's discrete dynamical system

Basic Newton's method (also known as the Newton-Raphson method) is one of the most influential methods for finding the roots of a real-valued polynomial $p(x)$ [58].

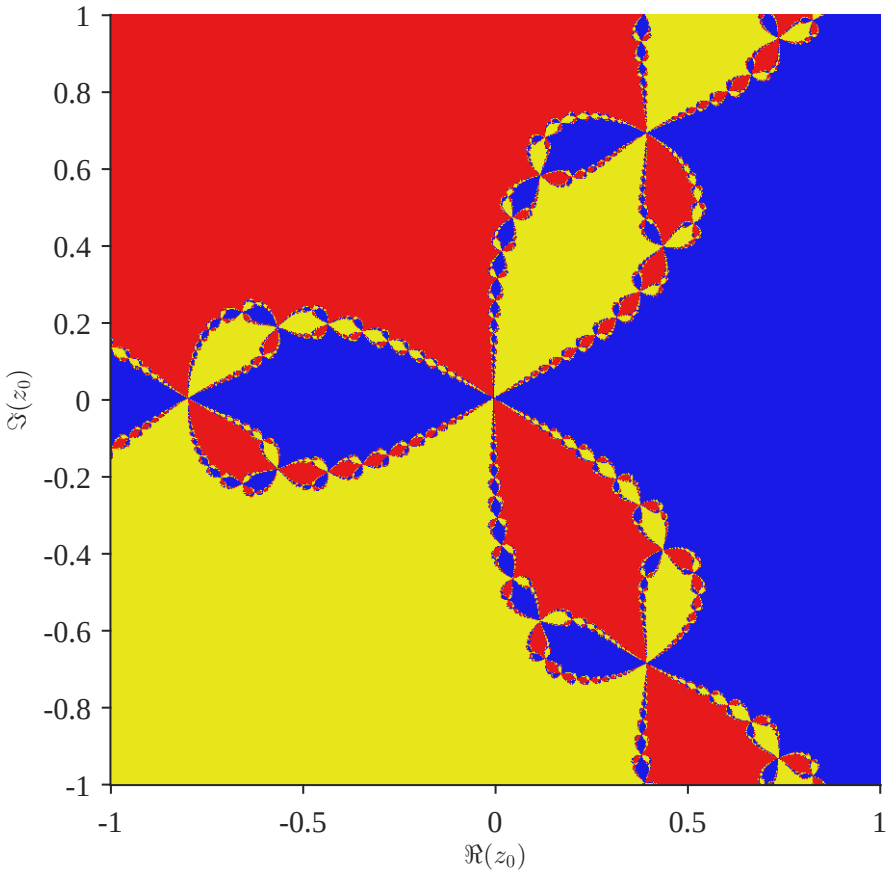

Figure 2.1: Basins of attraction for the NDDS with $p(z) = z^3 - 1$. Each color corresponds to the different attractor $\mathcal{A}_k$, where $k \in \{ 1, 2, 3 \}$.

After the method was established in the seventeenth century, modern interpretations and implementations began to differ substantially from the original version (see subsection 2.1.4 for various applications).

In the nineteenth century Schröder [59] and Cayley [60] came up with problems and solutions that eventually led to the formal generalization of the Newton's method for a polynomial $p(z)$ with complex coefficients. In this work it is referred to as the Newton's discrete dynamical system.

2.1.1. Introduction to Newton's discrete dynamical system

A Newton's dynamical system $f : \mathbb{C} \to \mathbb{C}$ is a discrete dynamical system fully described by its iterations $z_{k+1} = f(z_k)$, where $z_k, z_{k+1} \in \mathbb{C}$.

Definition 2.1. For a given complex polynomial $p(z)$ a single **Newton's iteration** at a point $z \in \mathbb{C}$ is defined as

$$f_p(z) = z - \frac{p(z)}{p'(z)}. \tag{2.1}$$

Once the evolutionary process is fully described, the discrete Newton's dynamical system (NDDS for short) corresponding to some complex polynomial $p(z)$ can be considered. The behavior of the aforementioned dynamical system is characterized by orbits $\{ z_0, z_1, z_2, \dots \}$. Each orbit is determined unambiguously by the initial seed $z_0 \in \mathbb{C}$ using the known iterative process

$$z_n = f_p^{\circ n}(z_0), \quad \forall n \in \mathbb{N}. \tag{2.2}$$

The emphasis on a general polynomial p is omitted during the further analysis. The third degree polynomial $p(z) = z^3 - 1$ is taken by default, unless specified otherwise.

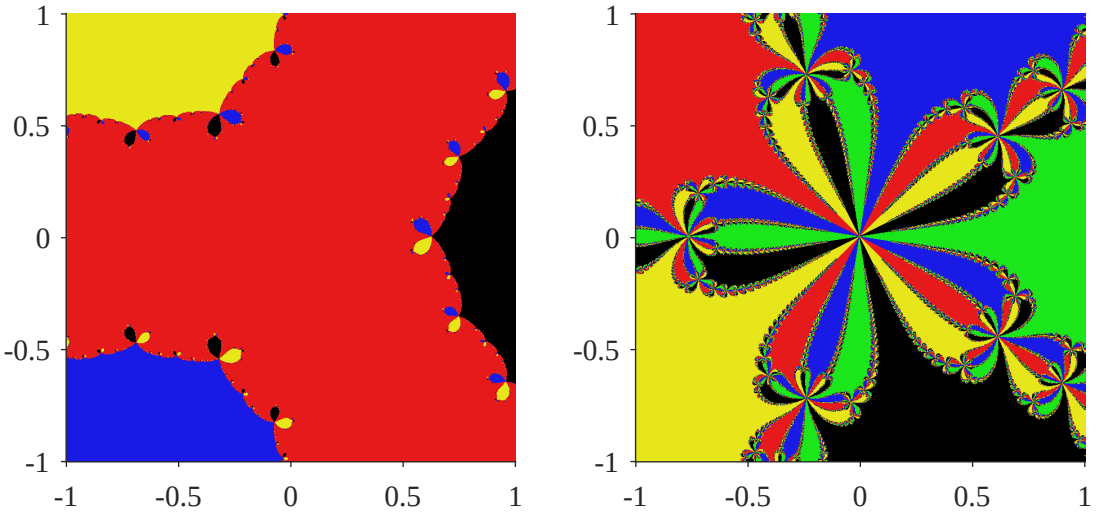

(a) $p(z) = z^4 - z$; **(b)** $p(z) = z^5 - 1$.

Figure 2.2: Basins of attraction for the NDDS with polynomials of higher order. Different polynomials $p(z)$ are used.

In figure 2.1 basins of attraction $\mathcal{B}_k$, where $k \in \{ 1, 2, 3 \}$, of the NDDS are calculated and presented visually using the default polynomial $p(z) = z^3 - 1$. It is apparent that the basins are intertwined in a complex manner and further investigations are needed.

Polynomials of higher order $p(z) = z^4 - z$ and $p(z) = z^5 - 1$ are also assigned to NDDS and presented visually in figure 2.2. In this case similarly complex processes are observed near the boundary of basins $\partial\mathcal{B}$.

A variation of escape time algorithm (see subsection 1.3.3) is used for calculations. The appropriate attractor is assigned to an initial seed $z_0 \in \mathbb{C}$ after $n = 30$ iterations.

2.1.2. Properties of Newton's discrete dynamical system

Attractors

Newton's discrete dynamical system f_p has some attractors $\mathcal{A} \subset \mathbb{C}$, provided that the polynomial p is non-constant. The set of attractors comprises the fixed points satisfying the definition $\{\, r \in \mathbb{C} \mid p(r) = 0 \,\}$. Consequently, it is important to understand the basins of attraction $\mathcal{B}$ for each attractor - the structure, properties and dynamics of these peculiar sets [61].

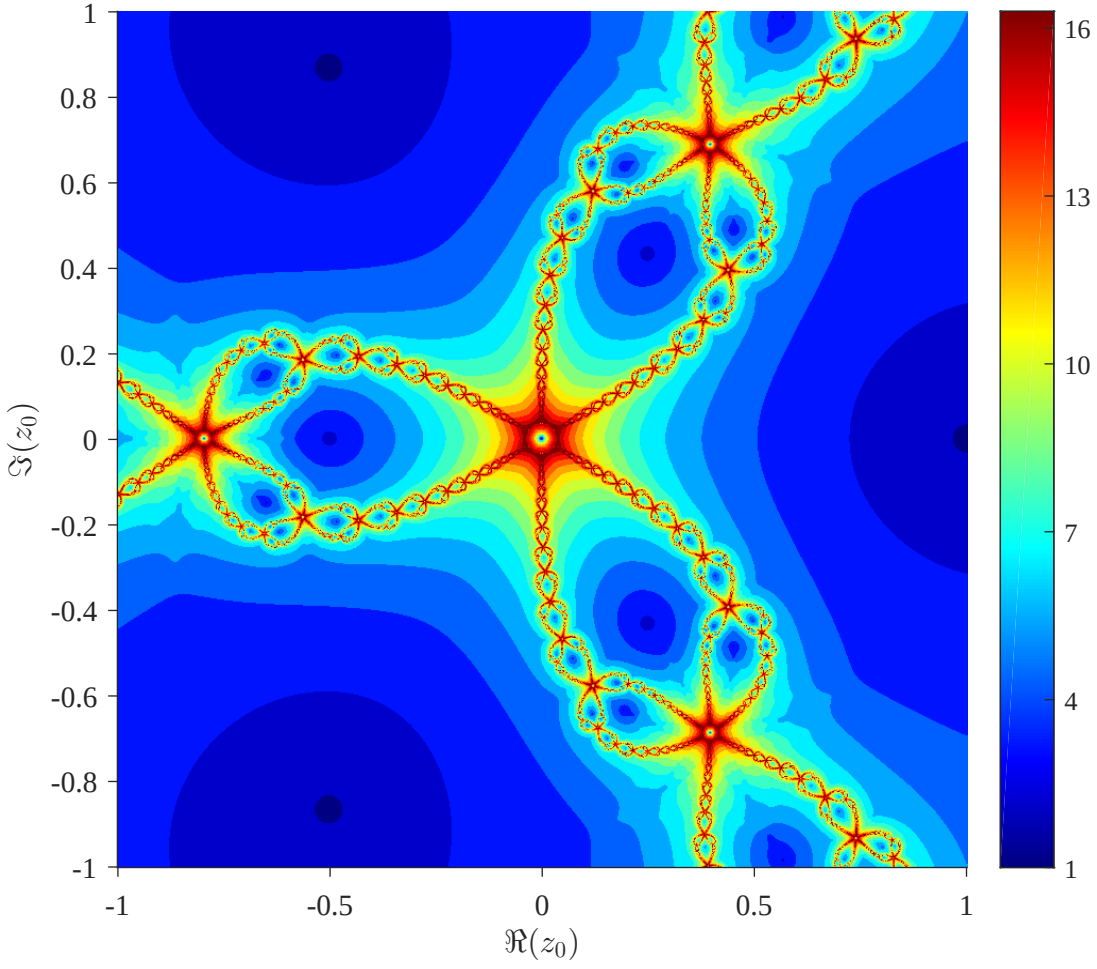

Figure 2.3: H-ranks for the NDDS with $p(z) = z^3 - 1$.

Basin boundaries

In the twentieth century Fatou [62] and Julia [63] made some independent discoveries regarding the basins of attraction $\mathcal{B}$ and especially the boundaries of these basins $\partial\mathcal{B}$ that are present in NDDS. If there are multiple Fatou domains (basins) $F_k = \mathcal{B}_k$, for some $k = \overline{1, \ldots, n}$, then each

point of the Julia set (boundary) $J = \partial\mathcal{B}$ must contain points from multiple basins in its neighborhood. If there are more than two different basins of attraction $n > 2$, then the Julia set is not a simple curve but rather a fractal shape $J = \mathcal{F}$ [2].

Speed of convergence

Another important aspect is the speed of convergence that is characterized by H-ranks. In figure 2.3 Hankel ranks are calculated using the default polynomial $p(z) = z^3 - 1$. Since the convergence of a Julia set J cannot be predicted, Hankel ranks are substantially higher in the vicinities of the basin boundary $\partial\mathcal{B}$. It also shows that the system can be very sensitive to its choice of starting points outside of certain regions.

2.1.3. Generalization of Newton's discrete dynamical system

NDDS itself is a classical tool whose typical speed of convergence varies from quadratic to linear depending on initial conditions [64]. A more general case is considered in order to gain additional flexibility

$$f_p(z) = z - \alpha\frac{p(z)}{p'(z)}. \tag{2.3}$$

The modified Newtonian iteration (**2.3**) introduces an arbitrary coefficient $\alpha \in \mathbb{C}$ instead of a constant value $\alpha = 1$.

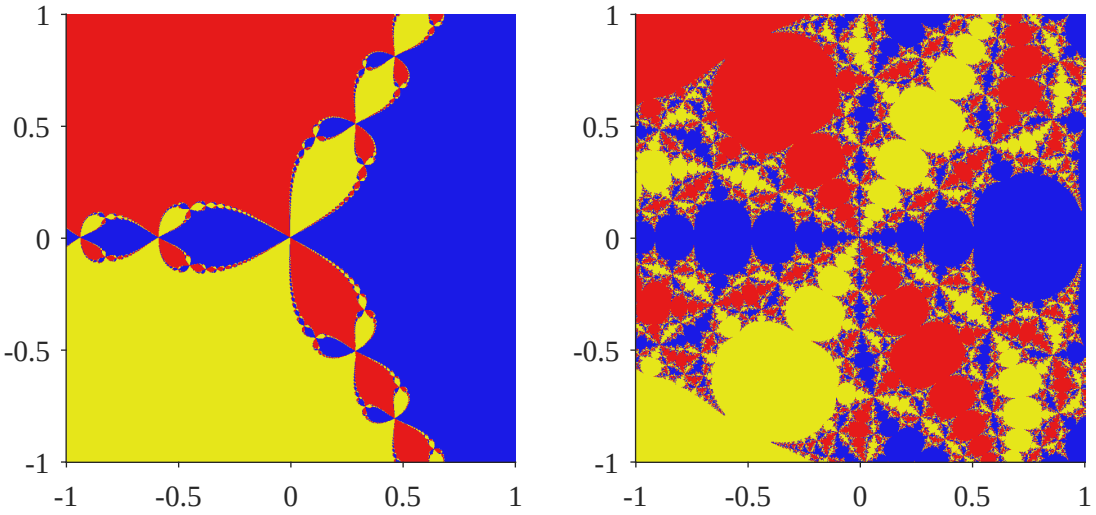

(a) $\alpha = 0.5$; **(b)** $\alpha = 2$.

Figure 2.4: Basins of attraction for the relaxed NDDS with $p(z) = z^3 - 1$. Different parameters $\alpha \in \mathbb{R}$ are used.

This generalization is called a relaxed Newton's discrete dynamical system [65]. It introduces a quantitative change in the speed of convergence as well as a qualitative change in the basins of attraction for the NDDS, even for $\alpha \in \mathbb{R}$. Typically $0 < \alpha < 1$ softens the fractal pattern of the basin boundary while performing smaller changes in variable during every iteration (see fig. 2.4a). On the other hand, $\alpha > 1$ typically sharpens the fractal pattern while providing bigger and more aggressive changes in variable (see fig. 2.4b). Overall this effect can be clearly seen in figure 2.4.

2.1.4. Applications of Newton's discrete dynamical system

NDDS can be used to analyze dynamical systems of varying degree of difficulty. In [64] Newton's method is considered as an iterative scheme to compute the complicated basins of attraction for some discrete dynamical systems. The chaotic number of iterations needed by Newton's method to converge to its attractors is discussed in [66]. A general behavior of Newton's method for cubic polynomials is investigated in [67], including the emergence of period-three orbits.

The emergence of fractals in NDDS is well-acknowledged amongst contemporary researchers. Both theoretical and experimental evidence of fractal characteristics of Newton's method is presented in [3]. Another overview of Newton's method and the convergence to fractal patterns is published in [68]. Some peculiar examples of fractals obtained using Newton's method are presented in [69]. The theory for stabilization of Newton's method in order to eliminate fractal basin boundaries is developed in [70]. Implications of the fractal basin boundaries generated by Newton's method for the aero-elastic analysis of a helicopter motion is discussed in [71].

Complicated relations between the basins of attraction lead to peculiar applications. An in-depth analysis of interwoven basins of attraction using a damped Newton's method is discussed in [72]. A graphical presentation of interlacement amongst three different basins of attraction is Newton's method is presented in [73].

A variety of alternatives and modifications to Newton's method are known. A modification of Newton's method using some novel adaptive step size control procedure is proposed in [74]. Standard Newton's method, Halley's method, and Schroder's method is compared in terms of structural characteristics of Julia sets in [75]. A variety of different possible generalizations of Newton's method is reviewed in [65].

2.2. Fractal dimension

2.2.1. Introduction to fractal dimension

For a lot of usual and familiar objects the notion of dimensionality is very intuitive and straightforward. For example, a manifold is D-dimensional if locally it resembles a Euclidean space of dimension D, which obviously has an integer value [76]. However, sometimes an object does not conform to any integer dimension. In that case, some more general tools are needed in order to understand and evaluate the dimension.

Ideally, a generalized definition of dimension D should satisfy the following requirements:

1. Points as well as countable unions of points X have $D(X) = 0$.
2. Manifolds M have an integer dimension $D(M) \in \mathbb{N}$ which coincides with the usual notion of topological dimension.
3. General sets $\mathcal{F}$ may have some fractional dimension $D(\mathcal{F}) \notin \mathbb{Z}$.

Unfortunately, it can be exceptionally hard to determine the precise fractal dimension of a given entity $\mathcal{F}$ in general case. Numerical approximations are typically used instead. The following subsections are dedicated to this matter in order to give some deeper insights regarding the problem.

2.2.2. Concept of fractal dimension

There are multiple characteristics that may be referred to as fractal dimensions. These measures provide an objective means to compare sets in terms of various features.

Box counting dimension (also known as Minkowski or Minkowski–Bouligand dimension) provides a way of determining the fractal dimension of a set $\mathcal{F}$ in any metric space. However some more preliminary definitions are necessary before further introduction.

Definition 2.2. The **box** of side length ε around the point $z_0 \in \mathbb{C}$ is defined

$$B(\varepsilon, z_0) = \left\{ z \in \mathbb{C} \,\middle|\, \Re(z_0) - \frac{\varepsilon}{2} \leq \Re(z) \leq \Re(z_0) + \frac{\varepsilon}{2}, \Im(z_0) - \frac{\varepsilon}{2} \leq \Im(z) \leq \Im(z_0) + \frac{\varepsilon}{2} \right\}. \quad \textbf{(2.4)}$$

The box defined above is actually a closed ball described using Manhattan metric [77] instead of a more typical Euclidean one. Nevertheless, it is useful when working in discrete grids which typically occur in computational environments.

Definition 2.3. The **minimal number of boxes** of side length ε that are needed to cover a given closed and compact set $\mathcal{F}$ is denoted

$$N(\varepsilon) = \min \left\{ n \in \mathbb{N} \,\middle|\, \mathcal{F} \subset \bigcup_{k=1}^{n} B(\varepsilon, z_k), z_k \in \mathbb{C} \right\}. \quad \textbf{(2.5)}$$

Such a number will always be found in case of $\mathcal{F}$ being compact because it follows from the very definition of compactness that there exists a finite subcover of (open) balls. Amongst these well-defined and finite coverings some (or at least one) will be minimal.

Now a particular proposed dimension D is related to the number N such that

$$N(\varepsilon) \approx C\varepsilon^{-D}, \quad \text{for some } C > 0; \quad \textbf{(2.6)}$$

and the above approximation becomes more precise as the multiplier ε decreases. Then it is natural to solve for D by taking the logarithm to the base e and obtain

$$D \approx \frac{\log N(\varepsilon) - \log C}{\log(1/\varepsilon)}. \quad \textbf{(2.7)}$$

Since the evaluation of dimension in question involves counting the number of ε-sized boxes $N(\varepsilon)$, it suffices to have a reasonable approximation of $\mathcal{F}$ and work at a fine precision ε. Then the second summand in the numerator of (**2.7**) disappears and this leads to the following definition.

Definition 2.4. The **box counting dimension** (or simply dimension) D of a compact non-empty set $\mathcal{F} \subset \mathbb{C}$ is defined as

$$D(\mathcal{F}) = \lim_{\varepsilon \to 0} \frac{\log N(\varepsilon)}{\log(1/\varepsilon)}; \tag{2.8}$$

where $N(\varepsilon)$ is the number of ε-sized boxes that are required to cover $\mathcal{F}$. □

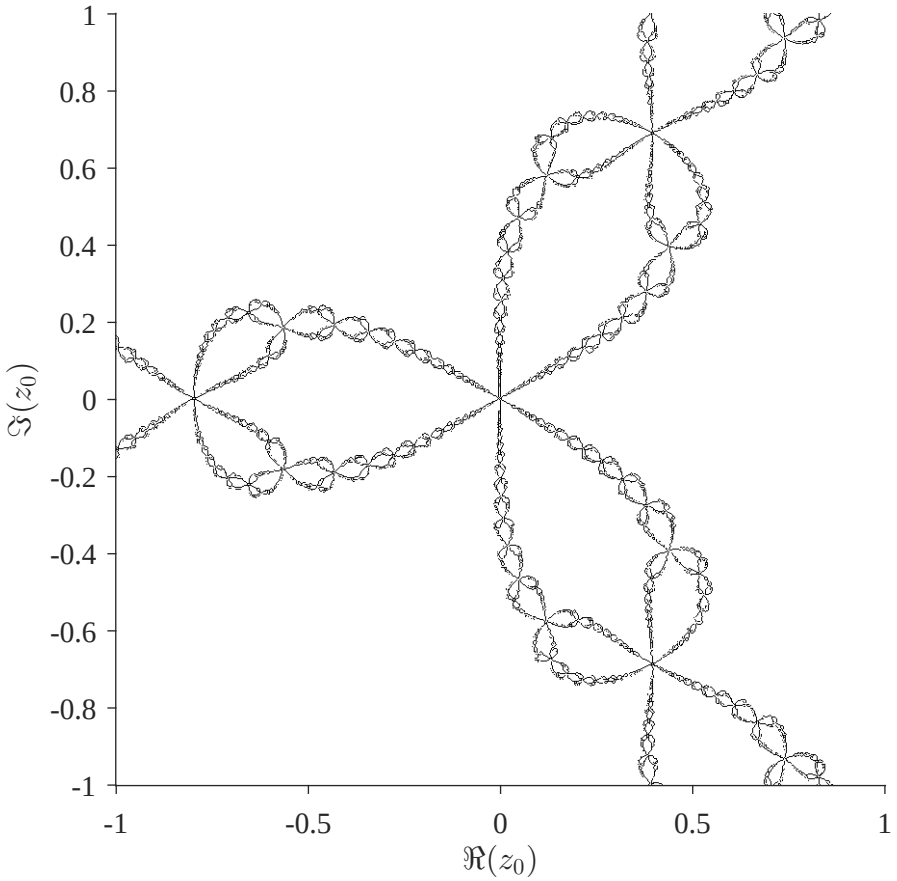

Figure 2.5: Basin boundary $\mathcal{F} = \partial\mathcal{B}$ for the NDDS with $p(z) = z^3 - 1$.

It is possible to extend the definition 2.4 and provide a value of dimension for a wider variety of sets. It is possible to use the following superior limit

$$D(\mathcal{F}) = \limsup_{\varepsilon \to 0} \frac{\log N(\varepsilon)}{\log(1/\varepsilon)}. \tag{2.9}$$

It can be proved that the above two presentations (**2.8**) and (**2.9**) are mathematically consistent [43]. However, the latter is obviously more general. This broader definition (**2.9**) can be applied in some more complicated cases where the first one fails. However, in the scope of this work it is sufficient to use the former approach (**2.8**).

Example 2.1. Let's consider a unit square $\mathcal{F} = \{\, z \in \mathbb{C} \mid 0 \leq \Re(z) \leq 1, 0 \leq \Im(z) \leq 1 \,\}$ which intuitively has dimensionality equal to 2. Take a decreasing positive sequence

$$\left(1 \quad 1/2 \quad 1/4 \quad \ldots \quad 1/2^n \quad \ldots\right).$$

It is understandable that for this set $\mathcal{F}$ the associated box counts

$$\begin{aligned} &N(1) = 1, \\ &N(1/2) = 4, \\ &N(1/4) = 16, \quad \text{and generally} \\ &N(1/2^n) = 4^n. \end{aligned}$$

The expression (**2.8**) is applied in order to obtain the fractal dimension

$$D(\mathcal{F}) = \lim_{n \to +\infty} \frac{\log N(1/2^n)}{\log(2^n)} = \lim_{n \to +\infty} \frac{\log(4^n)}{\log(2^n)} = \frac{\log 4}{\log 2} = 2.$$

Example 2.2. It can be approximated using the box counting algorithm (see [61]) that the fractal dimension of the basin boundary seen in figure 2.5 is equal to $D(\mathcal{F}) = 1.437$.

2.2.3. Algorithm to approximate fractal dimension

In short, the conventional idea of approximation involves scanning a non-overlapping ε-sized grid, finding the portions containing $\mathcal{F}$, and making conclusions according to the definition of box counting dimension.

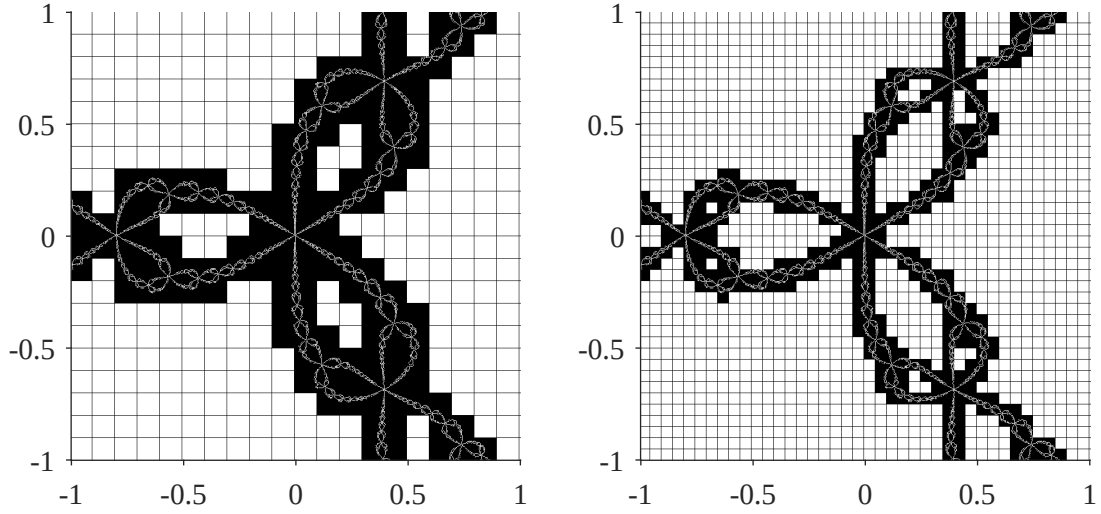

(a) $\varepsilon = 0.1;\ N(\varepsilon) = 145;$ **(b)** $\varepsilon = 0.05;\ N(\varepsilon) = 355.$

Figure 2.6: The principle of box counting using boxes of various sizes ε. The digital representation of $\mathcal{F}$ is split into an ε-grid, then count the nodes where the basin boundary $\partial\mathcal{B}$ is present.

In reality the ability to reduce ε is limited. For digital images (the representation of fractal structures) it is not possible to zoom more than to an individual pixel. The proposed solution:

1. Look at some finest $\varepsilon \in S$ values.
   These should initially cover 1×1 grid of pixels, then 2×2 grid pixels and so on (see fig. 2.6).

2. Calculate the observations $\log N(\varepsilon)$ and $\log(1/\varepsilon)$ in each case.
   This step is self-explanatory. The definition 2.3 is applied.

3. Approximate the slope using the least square linear regression or an alternative method.
   Assume that some pairs of observations (x_k, y_k), $k = \overline{1, \ldots, n}$, are supposed to be related $y_k = \gamma x_k + C$ up to some level of disturbance. Here γ is the slope and C is the constant term. Then the evaluations that minimize root-mean-square error (RMSE) are

$$C = \frac{\sum_{k=1}^{n} y_k - \gamma \sum_{k=1}^{n} x_k}{n}; \tag{2.10}$$

$$\gamma = \frac{n \sum_{k=1}^{n} (x_k y_k) - (\sum_{k=1}^{n} x_k)(\sum_{k=1}^{n} y_k)}{n \sum_{k=1}^{n} x_k^2 - (\sum_{k=1}^{n} x_k)^2}. \tag{2.11}$$

   After aforementioned procedures the approximation of fractal dimension D may be expressed

$$D(\mathcal{F}) \approx \frac{|S| \sum_{\varepsilon \in S} \log N(\varepsilon) \log(1/\varepsilon) - \left(\sum_{\varepsilon \in S} \log N(\varepsilon)\right) \cdot \left(\sum_{\varepsilon \in S} \log(1/\varepsilon)\right)}{|S| \sum_{\varepsilon \in S} \log^2(1/\varepsilon) - (\sum_{\varepsilon \in S} \log(1/\varepsilon))^2}. \tag{2.12}$$

This approximation is used in further research and analysis.

2.2.4. Applications of fractal dimension

Many various real-world phenomena exhibit some fractal properties. These properties are well described using the concept of fractal dimension. In neuroscience, different cell types apparently have significantly different dimensions [78]. In medicine, the dimension is useful for studies of X-ray and MR images [79]. Overall, the fractal dimension is an important tool for studies of natural patters and textures [80].

On the other hand, applications of fractal dimension are directly related to applications of fractals themselves. These aspects are discussed in detail in subsection 1.3.4.

2.3. Wada measure

2.3.1. Introduction to Wada characteristic

In theoretical mathematics, there exists a concept called lakes of Wada. It occurs in a plane which is divided into three disjoint connected open sets that have a peculiar and highly counterintuitive property: they all share the same boundary.

In applied mathematics, there exists a variety of vastly different nonlinear dynamical systems describing both natural and unnatural phenomena. Typically, these systems possess multiple nontrivial attractors. It is therefore understandable that the principles of Wada are defined in terms of basins of attraction and their respected boundaries, which are shared.

Example 2.3. Let's construct a region that has full Wada property. For that purpose, three different basins of attraction R, Y, B are used. The basins correspond to colors red, yellow and blue respectively.

1. Without loss of generality it can be said that the region is rectangular.
   Initially all points in the region are undefined (not assigned to any basin of attraction).

2. The undefined region is divided vertically into three equal parts.
   Side parts are assigned to two different basins of attraction; the middle part is left undefined.

3. The undefined parts are divided vertically into three equal even smaller parts.
   Side parts are left undefined; the middle part is assigned to the basin which is not nearby.

4. Step 3 is repeated indefinitely.

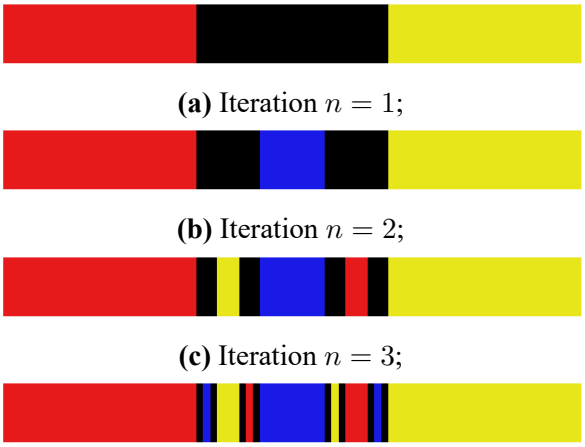

(a) Iteration $n = 1$;

(b) Iteration $n = 2$;

(c) Iteration $n = 3$;

(d) Iteration $n = 4$.

Figure 2.7: Emergence of Wada property. A region is divided into three pieces, side pieces are assigned to two different basins of attraction, the middle piece is undefined. In every subsequent turn an undefined portion is again divided into three pieces, side pieces are undefined, the middle piece is assigned to the basin of attraction which is not nearby.

As the number of repeated iterations n increases, the set of undefined points is getting smaller. In the limit case $n \to +\infty$, a whole region of points is assigned to some basins R, Y, B. Moreover, all these basins have a common boundary, thus the full Wada property. The whole process is illustrated in figure 2.7.

2.3.2. Concept of Wada measure

As already discussed, the situation when every boundary point neighbors more than two distinct basins of attraction $\mathcal{B}_k$, $k \in \overline{1, \ldots, n}$, is known as the Wada property [81]. If the system has exactly three different attractors $\mathcal{A}_1,\ \mathcal{A}_2,\ \mathcal{A}_3$, it follows that all basins of attraction $\mathcal{B}_1,\ \mathcal{B}_2,\ \mathcal{B}_3$ have a common boundary $\partial\mathcal{B}$. Some more preliminary definitions are needed before proceeding with quantitative approximations of Wada measure.

Definition 2.5. The **number of n-boxes** $N_n(\varepsilon)$ is the minimal number of boxes (according to the definition 2.3) that satisfy an additional property

$$B(\varepsilon, z) \cap \mathcal{B}_k \neq \varnothing, \quad \text{for all } k \in \{ k_1, k_2, \ldots, k_n \}; \tag{2.13}$$

for a fixed side length ε and compact nonempty set $\mathcal{F}$. □

Simply put, the number of n-boxes counts the size of (partial) $\mathcal{F}$ covering which contains points from at least n different basins of attraction. Then the following inequality holds

$$0 \leq N_n(\varepsilon) \leq N(\varepsilon), \quad \forall n \in \mathbb{N},\ \forall \varepsilon > 0. \tag{2.14}$$

Let's look at the case where a given dynamical system has exactly three attractors and three corresponding basins of attraction $\mathcal{B}_1,\ \mathcal{B}_2,\ \mathcal{B}_3$ more closely. In extreme cases where the basins are relatively far away and form distinct boundaries it is reasonable to expect $N_3(\varepsilon) \approx 0$, whereas if basins are intertwined and close together it should be $N_3(\varepsilon) \approx N(\varepsilon)$.

Finally, the Wada measure can be defined with precision.

Definition 2.6. A **Wada measure** W for a compact non-empty set $\mathcal{F} \subset \mathbb{C}$ is defined as

$$W(\mathcal{F}) = \lim_{\varepsilon \to 0} \frac{N_3(\varepsilon)}{N_2(\varepsilon)} = \lim_{\varepsilon \to 0} \frac{N_3(\varepsilon)}{N(\varepsilon)} \tag{2.15}$$

where $N(\varepsilon)$ and $N_3(\varepsilon)$ is the number of ε-sized boxes that cover $\mathcal{F}$. □

In terms of the classical theory of probability, the Wada measure is the probability of a random point taken from boundary $\partial\mathcal{B}$ having at least three different basins of attraction in its immediate neighborhood. If the region of interest has full Wada property, then its boundary $\partial\mathcal{B}$ has a theoretical Wada measure $W(\partial\mathcal{B}) = 1$. On the contrary, if the region does not resemble Wada situation at all, then $W(\partial\mathcal{B}) = 0$.

2.3.3. Algorithm to approximate Wada measure

Once again, the idea involves scanning a non-overlapping ε-sized grid, finding the portions containing $\mathcal{F}$, counting the number of basins of attraction that they contain, and making conclusions according to the definition of Wada measure.

The ability to reduce ε is similarly limited to no more than an individual pixel. The proposed solution is this:

1. Look at some finest $\varepsilon \in S$ values.
   These should initially cover 2×2 grid of pixels, then 3×3 grid pixels and so on (see fig. 2.8).

2. Calculate the observations $N(\varepsilon)$ and $N_3(\varepsilon)$ in each case.
   The empirical probability of any given box being a 3-box is $N_3(\varepsilon)/N(\varepsilon)$.

3. Take the mean empirical probability of the observations.

After aforementioned procedures the outcome may be expressed as

$$W(\mathcal{F}) \approx \frac{1}{|S|} \sum_{\varepsilon \in S} \frac{N_3(\varepsilon)}{N(\varepsilon)}. \tag{2.16}$$

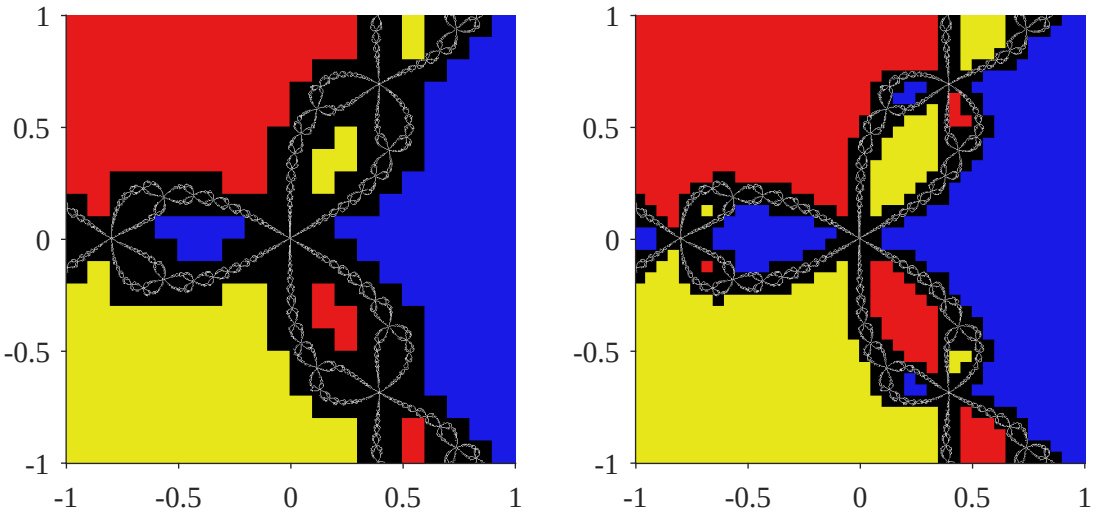

(a) $\varepsilon = 0.1;\ N_3(\varepsilon) = 143;\ N(\varepsilon) = 145;$ **(b)** $\varepsilon = 0.05;\ N_3(\varepsilon) = 342;\ N(\varepsilon) = 355.$

Figure 2.8: The principle of Wada measure using boxes of various sizes ε. The digital representation of $\mathcal{F}$ is split into an ε-grid, then count the nodes where the basin boundary $\partial\mathcal{B}$ is present and count the occurrences from different basins of attraction.

Realistically, the approximated value of $W(\mathcal{F})$ is never quite equal to 1. On the other hand, it serves its purpose of measuring and comparing Wada characteristics of different dynamical systems and situations. This approximation is mainly used in further research and analysis.

2.3.4. Applications of Wada characteristic

Rigorous theorems and important statements regarding Wada basin boundaries and basin cells are presented in [82]. Wada property for different types of attractors including strange nonchaotic attractors is discussed in [83]. Sufficient and necessary conditions guaranteeing that three Wada basins are emerging from a tangent bifurcation are presented in [84].

Wada property emerges in a variety of systems of high interest in physics. Unpredictable behavior of Wada basin boundaries in the Duffing oscillator is noted in [85]. Wada property in some systems of chaotic scattering with multiple exit modes is analyzed in [86]. Topological characteristics, including Wada property, are considered for some systems of chaotic scattering in [87]. Fractal and – more specifically – Wada exit basin boundaries are analyzed in a tokamak system in [88].

Basins are highly interwoven even in non-standard situations. Seemingly unexpected situations where basins of attraction have Wada property are revealed in [81].

Wada effect is present in nature. Unpredictability of ecological models related to Wada basins is interpreted graphically in [89]. Examples of Wada characteristic in a periodically forced Lotka-Volterra predator-prey model are found in [90].

Modifications and generalizations of Wada quality are proposed by contemporary researchers. Transitions from totally Wada basins to partially Wada basins and vice versa are constructed in [91]. A novel method for testing for basins of Wada is proposed in [92].

Research

In this chapter that is dedicated to research the original numerical results and calculations are presented. All the following insights are directly related to the preliminaries, methods and mathematical tools described up to this point.

Section 3.1 reveals the analysis of basin boundaries. It is split into three important parts: analysis of dimensionality, Wada measure, and the relation between both of them.

Section 3.2 presents implications of chaos in the present setting. Once again it is divided into two subsections where different aspects are discussed. The first one considers the evaluation of uncertainty, the second one considers the control of the dynamical system.

3.1. Analysis of basin boundaries

Artificially generated visual representations of attractors and basins of attraction are amongst typical choices for researchers who seek to describe and analyze the behavior of some dynamical systems [93]. Therefore, it is important to do a quality presentation of characteristics that describe these basins of attraction, relations between aforementioned characteristics and possible implications of these results.

A scope of initial conditions $z_0 \in \mathbb{C}_1$ is considered. These are the conditions that belong to a complex square defined as $\mathbb{C}_1 = [-1, 1]^2$. This set includes all attractors for the default NDDS polynomial $p(z) = z^3 - 1$ and otherwise suits the needs of this work. Within the chosen scope values which are $|\Delta z| = 0.0025$ distance apart are evaluated, for example $-1, -0.9975, -0.995, \ldots, 1$. It is easy to see that after aforementioned discretization a 801×801-sized grid of possible values for z_0 is obtained.

Similarly, a scope of parameters $\alpha \in \mathbb{C}_1$ is considered. It is enough for the experiments because outside of this set the behavior of NDDS can be quite extreme and too rapid-changing for the delicate numerical analysis. Within the chosen scope some values which are $|\Delta\alpha| = 0.01$ distance apart are chosen, for example $-i, -0.99i, -0.98i, \ldots, i$. Once again, it is easy to see that after discretization a 201×201-sized grid of possible values for α is obtained.

Lastly, the number of iterations used in the model is $n = 30$. It corresponds to the depth of the trajectories $(z_0,\ z_1,\ z_2,\ \ldots,\ z_{30})$ and after z_{30} the orbit is assigned to the nearest attractor $\mathcal{A}$. It is possible to use a higher depth but the orbits tend to stabilize before n recalculations. Also the number of elements in the grid is limited anyway. Therefore, the benefits of significantly higher depth are questionable in the present setting.

3.1.1. Fractal dimension of basin boundaries

For the purposes of research the algorithm discussed in subsection 2.2.3 is used. In the process of approximation, different coverings ranging from 1×1 to 100×100 pixels are taken into account. This means $|S| = 100$ cases overall.

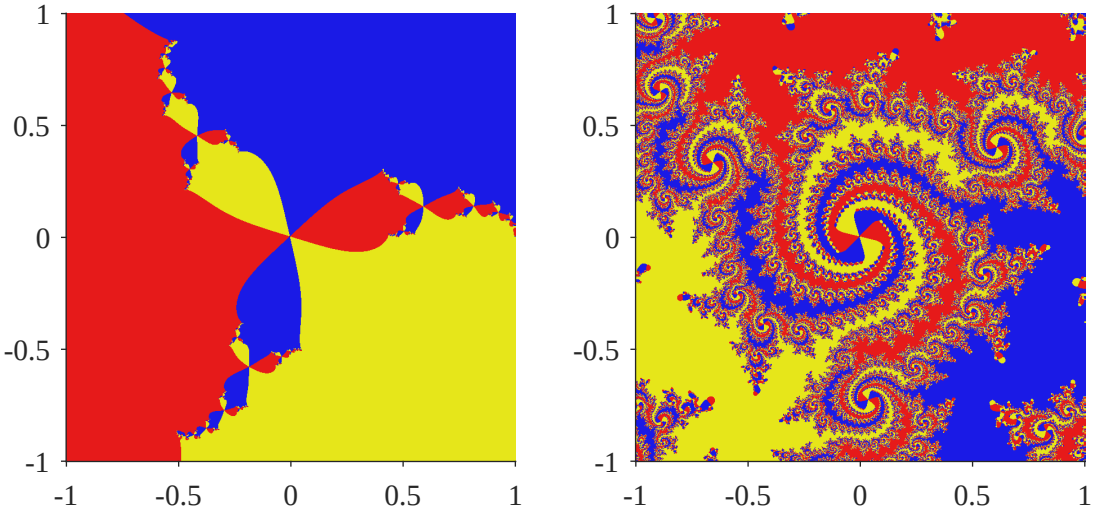

(a) $\alpha = -0.55 + 0.6i;\ D(\mathcal{F}_\alpha) = 1.21;$ **(b)** $\alpha = 0.5 + 0.9i;\ D(\mathcal{F}_\alpha) = 1.63.$

Figure 3.1: Basins of attraction for the relaxed NDDS with varying values of fractal dimension. Two different system parameters $\alpha \in \mathbb{C}$ are used.

In general, a fractal dimension D is a characteristic of complexity comparing how detail in a pattern changes with the scale at which it is being measured. For smooth simple curves this characteristic is a constant unit $D = 1$ meaning that there is no change in detail. But other possibilities exist. For example, let's take a particular parameter $\alpha = -0.55 + 0.6i$. Using the relaxed NDDS, its basins of attraction $\mathcal{B}$, basin boundary $\partial\mathcal{B} = \mathcal{F}$ and finally the corresponding fractal dimension $D(\mathcal{F}_\alpha) = 1.21$ is obtained. This result is quite different from, say, $\alpha = 0.5 + 0.9i$ and corresponding dimension $D(\mathcal{F}_\alpha) = 1.63$. The comparison can be seen visually in figure 3.1.

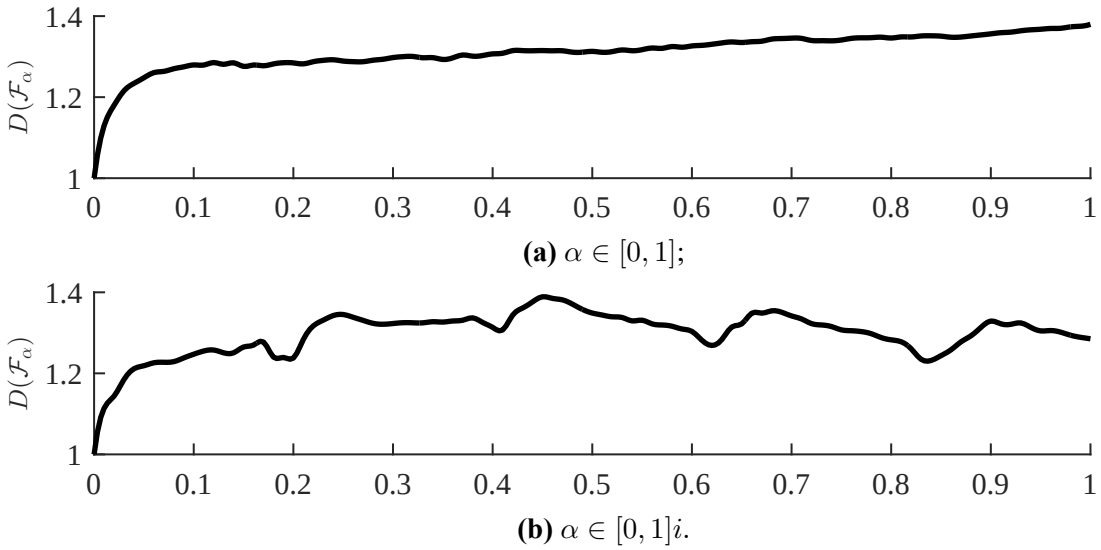

(a) $\alpha \in [0, 1];$

(b) $\alpha \in [0, 1]i.$

Figure 3.2: Fractal dimensions for the relaxed NDDS with varying parameter $\alpha \in \mathbb{C}$.

As the parameter α fluctuates starting from $\alpha = 0$, the changes in global characteristics are inspected. At this stage the aim of the procedure is to detect any possible peculiarities.

Initially some small positive constant $\varepsilon \approx 0.001$ is added so that $\alpha \in [0, 1]$. Beginning from $D(\mathcal{F}_0) \approx 1$ the fractal dimension increases almost monotonically until $D(\mathcal{F}_1) \approx 1.38$ and onwards (for example, $D(\mathcal{F}_2) \approx 1.60$). This effect can be clearly seen in figure 3.2 part (a).

Next, starting from the same $\alpha = 0$, some small imaginary constant $\varepsilon \approx 0.001i$ is added so that $\alpha \in [0, 1]i$. Effectively this creates a section of the parameter plane along the imaginary axis. But this time the dimension does not increase monotonically at all, see figure 3.2 part (b). Instead it demonstrates periodic-like behavior and has some local minima approximately at $\alpha \in \{\, 0.2i, 0.4i, 0.6i, 0.8i \,\}$. This is indeed a peculiar behavior that requires further investigation.

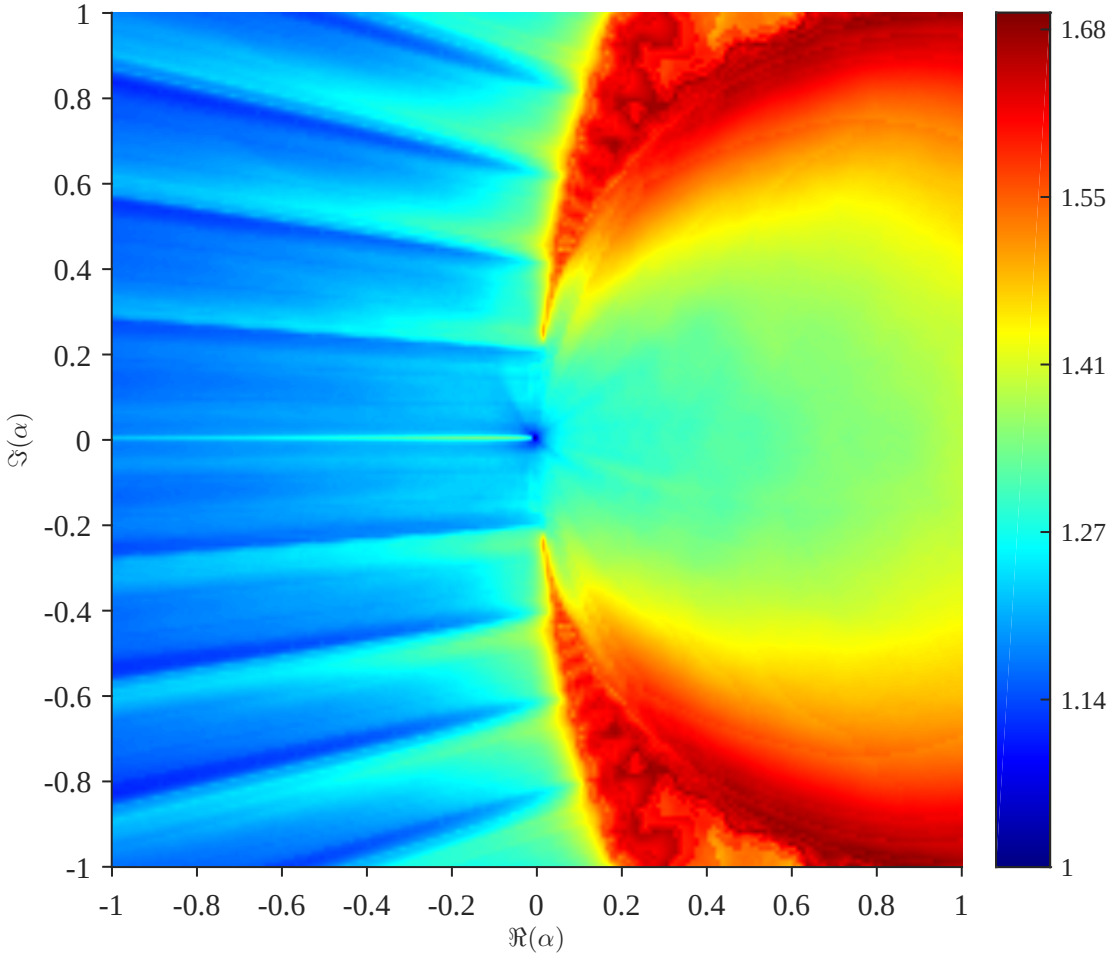

Figure 3.3: Fractal dimension $D(\mathcal{F}_\alpha)$ in the parameter plane $\alpha \in \mathbb{C}$.

Then some computationally-intensive calculations are performed for many more possible α values. As a result, fractal dimensions for the whole grid of parameter values is obtained. This result is presented in figure 3.3. It shows that the fractal dimension D is a highly non-trivial function of complex parameter $\alpha \in \mathbb{C}$ which apparently is symmetric with respect to the $\Im(\alpha) = 0$.

For $\Re(\alpha) \leq 0$, the dimensions tend to be relatively low, with the maximum being found to be $D(\mathcal{F}_{0.45i}) \approx 1.39$. The periodic-like behavior along imaginary axis is also present only in this semi-plane. Otherwise the imaginary part of the parameter α does not impact the observed dimension dramatically.

On the other hand, let's look at $\Re(\alpha) \geq 0$. In this semi-plane the dimensions vary substantially between $D(\mathcal{F}_0) \approx 1$ and $D(\mathcal{F}_{0.76+0.98i}) \approx 1.68$. The periodic-like behavior is not to be found here. As the $\Im(\alpha)$ approaches either ± 1, the observed dimension increases dramatically.

3.1.2. Wada measure of basin boundaries

The algorithm discussed in subsection 2.3.3 is used for the following part of this research. In the process of approximating Wada measure different coverings ranging from 2×2 to 101×101 pixels are taken into account (the single pixel case is trivial). This means $|S| = 100$ cases overall.

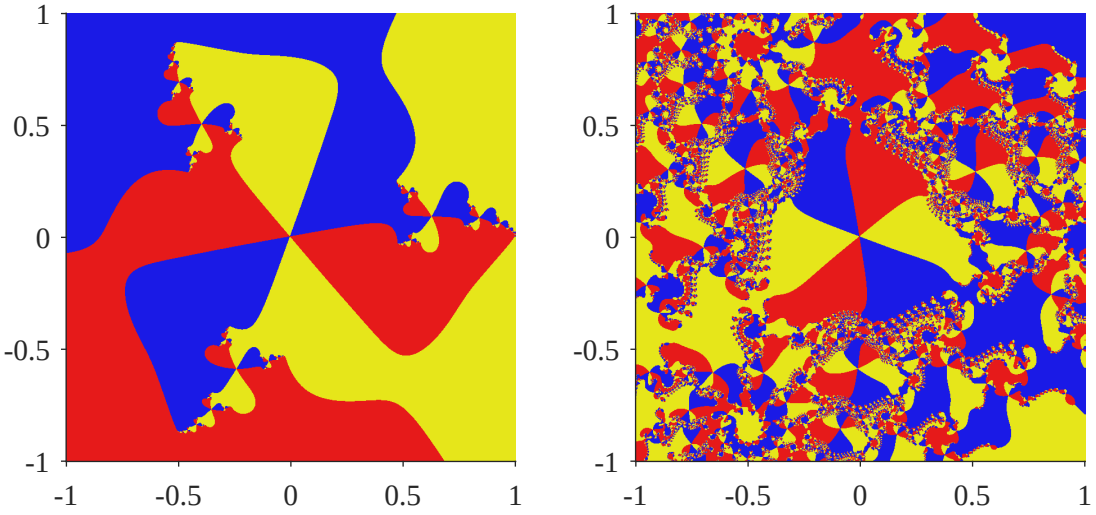

(a) $\alpha = -0.85 + 0.53i;\ W(\mathcal{F}_\alpha) = 0.28;$ **(b)** $\alpha = 0.1 + 0.6i;\ W(\mathcal{F}_\alpha) = 0.88.$

Figure 3.4: Basins of attraction for the relaxed NDDS with varying values of Wada measure. Different parameters $\alpha \in \mathbb{C}$ are used.

In general, Wada measure W indicates what percentage of boundary points $\mathcal{F}$ is neighboring more than two basins of attraction simultaneously. Naturally $W = 0$ corresponds to 0% while $W = 1$ corresponds to 100%.

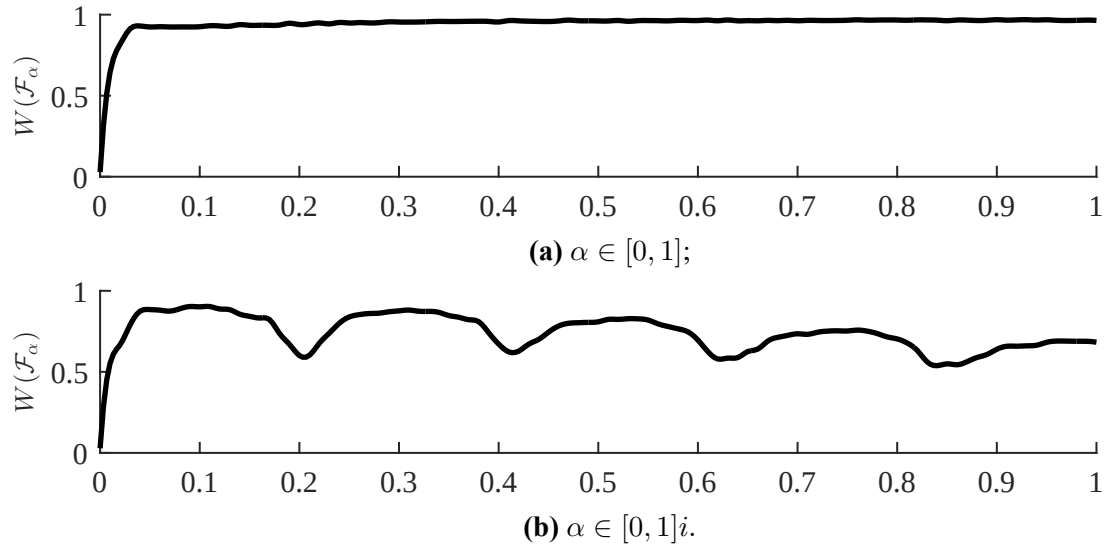

(a) $\alpha \in [0, 1];$

(b) $\alpha \in [0, 1]i.$

Figure 3.5: Wada measures for the relaxed NDDS with varying parameter $\alpha \in \mathbb{C}$.

For example, let's take a particular parameter $\alpha = -0.85 + 0.53i$. Using Newton's discrete dynamical system its basins of attraction $\mathcal{B}$, basin boundary $\partial\mathcal{B} = \mathcal{F}$ and finally the corresponding Wada measure $W(\mathcal{F}_\alpha) = 0.28$ is obtained. This result is very different from, say, $\alpha = 0.1 + 0.6i$ and corresponding measure $W(\mathcal{F}_\alpha) = 0.88$. The comparison is presented visually in figure 3.1.

As the parameter α varies in some direction starting from $\alpha = 0$, the changes in Wada measure are inspected. Some resemblance to fractal dimension is expected. However, it's worth emphasizing that Wada measure takes into account more data (basins of attraction themselves) compared to fractal dimension (only basin boundaries).

Initially some reasonably small positive constant $\varepsilon \approx 0.001$ is added so that $\alpha \in [0, 1]$. Beginning from $W(\mathcal{F}_0) \approx 0$ the Wada measure then increases rapidly until approximately $\alpha \approx 0.03$ when $W(\mathcal{F}_{0.03}) \approx 0.91$. Afterwards it stays at a similar level until the end of simulations when $W(\mathcal{F}_1) \approx 0.96$. This effect can be clearly seen in figure 3.5 part (a).

In another scenario, let's add some small imaginary constant $\varepsilon \approx 0.001i$ so that $\alpha \in [0, 1]i$. This creates a section of the parameter plane along the imaginary axis. This time the measure behaves in a very similar manner to fractal dimension, see figure 3.5 part (b). Namely it demonstrates periodic-like behavior and has some local minima approximately at $\alpha \in \{\, 0.2i, 0.4i, 0.6i, 0.8i \,\}$.

Overall this shows an expected resemblance compared to fractal dimension in one case (imaginary values), yet yields some new results in another scenario (real parameters).

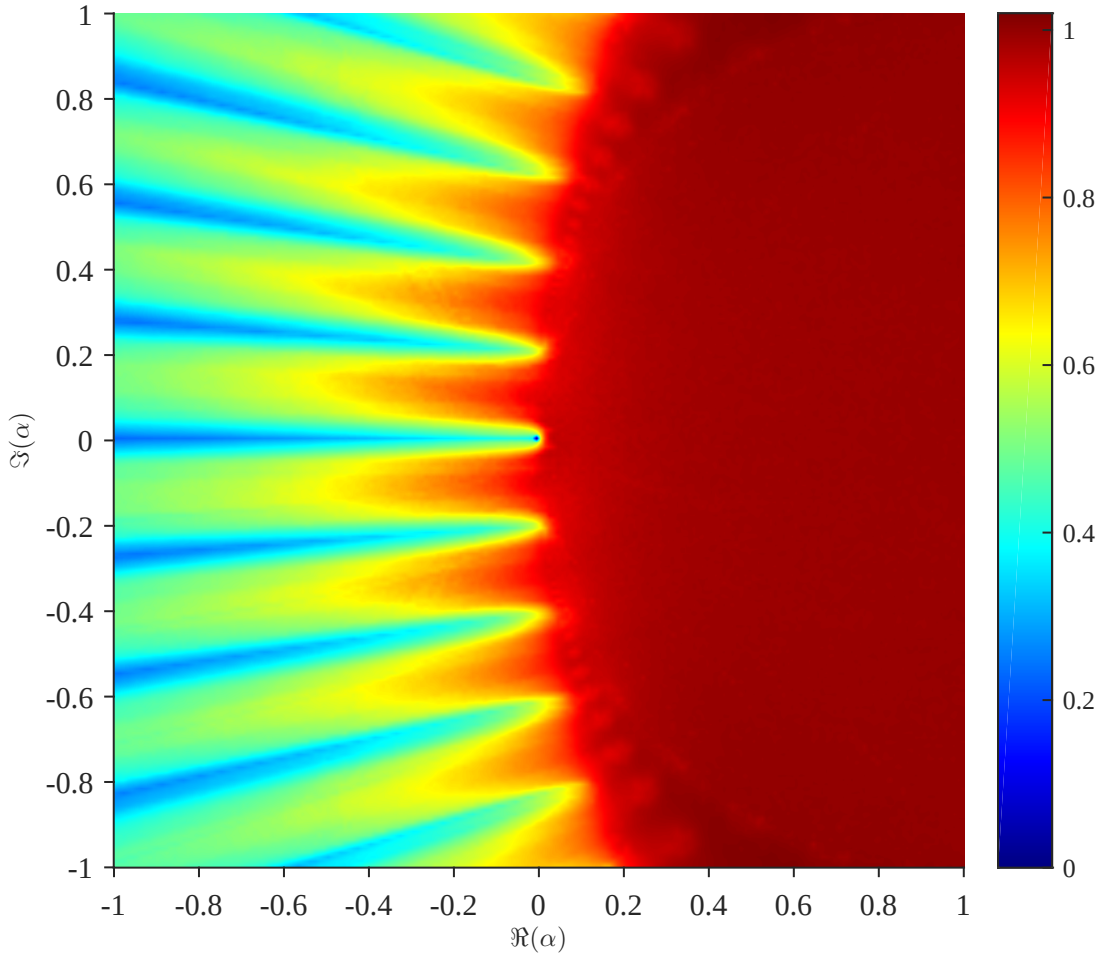

Figure 3.6: Wada measure $W(\mathcal{F}_\alpha)$ in the parameter plane $\alpha \in \mathbb{C}$.

Once again some computationally-intensive calculations for many more possible α values are performed. As a result, Wada measure for the whole grid of parameter values $\alpha \in \mathbb{C}_1$ is obtained. This obtained result is presented in figure 3.6. It shows that the Wada measure W is indeed a non-trivial function of complex parameter $\alpha \in \mathbb{C}$. It is also apparently the case that the characteristic $W(\mathcal{F}_\alpha)$ is invariant under $\alpha = x \pm iy$.

For $\Re(\alpha) \leq 0$, the Wada measures vary significantly within $W \in [0.03, 0.90]$. The average measure in this case is $\overline{W} \approx 0.53$. The periodic-like behavior along imaginary axis is present only in this semi-plane. This time the imaginary part of the parameter α can impact the observed measure noticeably.

On the other hand, let's look at $\Re(\alpha) \geq 0$. In this semi-plane the measure is relatively high. The highest observed value is $W(\mathcal{F}_{0.59-i}) \approx 0.99$. In fact the values are high almost everywhere except for $\Re(\alpha) \approx 0$ with average being $\overline{W} \approx 0.94$. Also the periodic-like behavior is not found and $\Im(\alpha)$ has no substantial impact on the observed Wada measures.

3.1.3. Relation between characteristics of basin boundaries

The results concerning fractal dimensions and Wada measures have been described separately. It was presented how and when these characteristics change within the family of basin boundaries. The logical follow-up is to integrate the two characteristics and present the joint results regarding the relation between both measures.

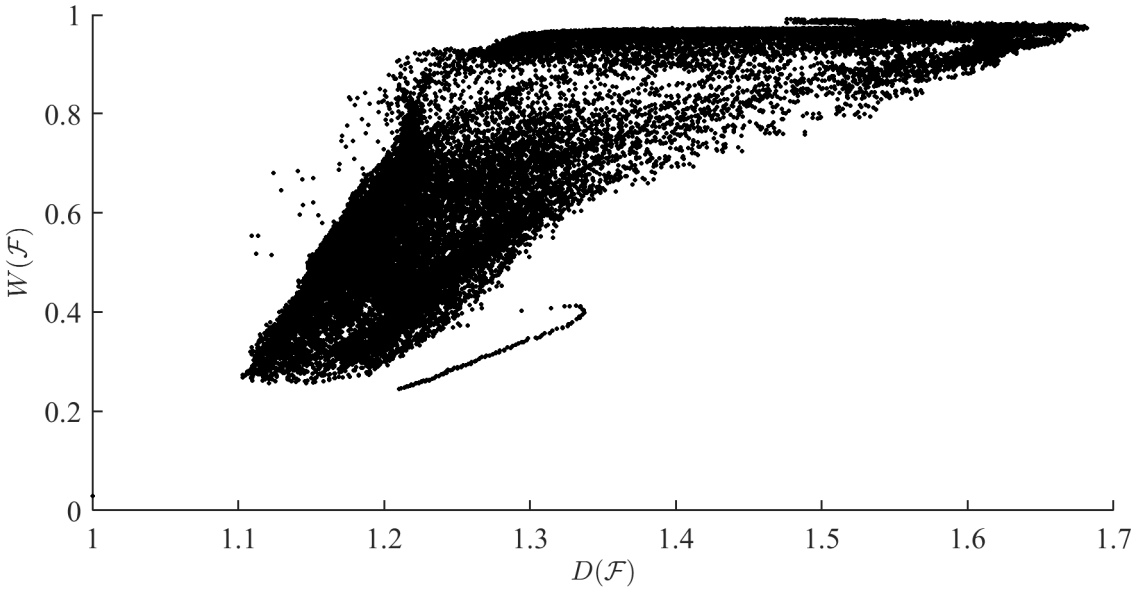

Figure 3.7: Fractal dimensions $D(\mathcal{F})$ and Wada measures $W(\mathcal{F})$ for all parameters $\alpha \in \mathbb{C}_1$.

Initially the scatter points are marked in figure 3.7 to plot the set of observations D and W for the data. Some tendencies can be noticed right away. Apparently there exists a positive correlation between the characteristics: the higher the fractal dimension D, the higher the Wada measure W. Different coefficients may be used to evaluate possible correlation:

1. Pearson's correlation coefficient measures the linear relationship between two continuous variables. The normality is not assumed nor checked. In fact only finite (co)variances are

assumed. The obtained outcome is

$$\rho_{D,W} = \frac{\overline{DW} - \overline{D} \cdot \overline{W}}{\sqrt{\overline{D^2} - \overline{D}^2}\sqrt{\overline{W^2} - \overline{W}^2}} = 0.82 \tag{3.1}$$

which indeed reveals a positive correlation.

2. Spearman's correlation coefficient measures the monotonic relationship between two continuous variables. The outcome is calculated very similarly, yet the measures themselves are replaced with ranks

$$r_{D,W} = \rho_{\text{rank}(D),\text{rank}(W)} = 0.87 \tag{3.2}$$

and once again a positive correlation is revealed. Because of ranking feature, the measure is relatively robust to outliers (unlike Pearson's correlation). It is possible that there exist some numerical outliers since the nature of the calculations is quite delicate.

Despite some positive correlation the relationship is still complex. It is possible to provide a sequence of fractal basin boundaries whose dimension D strictly increases, yet at the same time the corresponding Wada measure decreases. The aforementioned effect can be demonstrated in the scatter plot (see figure 3.7) by selecting a negatively correlated subset of observations ($\rho \approx -1$).

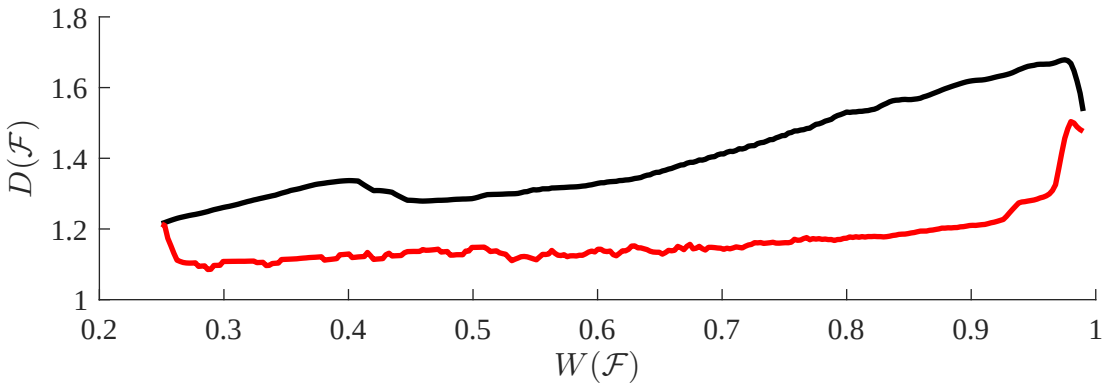

Figure 3.8: Minimum and maximum fractal dimensions for the ε-neighborhoods of a fixed Wada measure $W(\mathcal{F})$.

Now in figure 3.8 it is checked what fractal dimensions D exist when a particular Wada measure W is fixed. It is actually possible to find relatively low fractal dimensions $D < 1.2$ for (almost) all Wada measures $W < 0.9$. Afterwards when $W \geq 0.9$ the minimal dimension D is necessarily higher within the scope of parameters $1.2 \leq D < 1.6$. On the other hand, the maximal dimension increases along with fixed Wada measure with few exceptions in the present setting.

These observations can also be presented the other way around. For example, once the complex patterns have $D > 1.2$, a substantial Wada measure is expected as well - otherwise there would be no matches.

3.2. Implications of chaos

3.2.1. Uncertainty of the final attractor

In order to check the underlying uncertainty of the final attractor the setting of the NDDS is fixed as described below. The initial seeds belong to a grid of values around $z_0 = -0.793$ within the radius of $|\Delta z_0| = 0.01$. To ensure that there are enough simulations the distance between nodes in the grid has to be sufficiently small, around $\varepsilon \approx 0.0006$. This leads to the total number of simulations being $s = 795$ which is considered to be enough for reliable results.

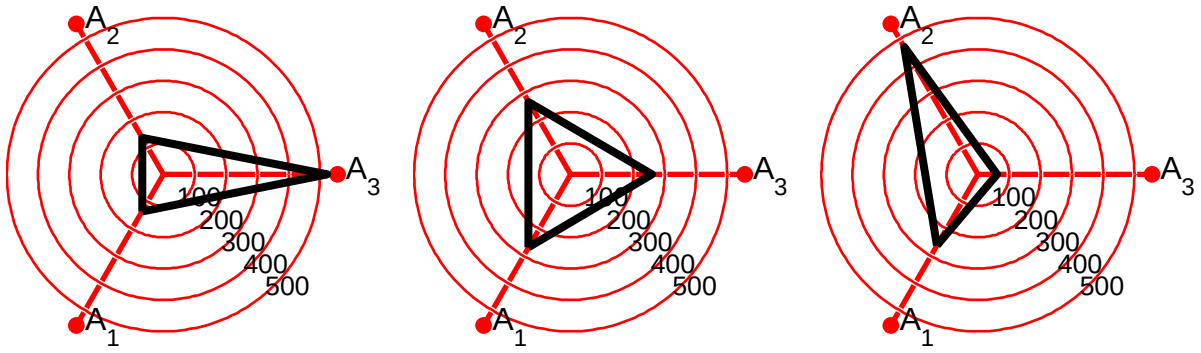

(a) $\alpha = 0.97$; **(b)** $\alpha = 1$; **(c)** $\alpha = 1 + 0.005i$.

Figure 3.9: Uncertainty of the final attractor when the initial seed $z_0 = -0.793$ fluctuates within $|\Delta z_0| = 0.01$ and the parameter α is slightly perturbed.

Initially the control parameter $\alpha = 0.97$ is set. It leads to the emergence of slightly smoothed basin boundary. After running the simulations, it is noticeable that the outcomes are quite tendentious: 523 cases converge to the attractor $\mathcal{A}_3$ while the other two $\mathcal{A}_1$ and $\mathcal{A}_2$ attract $s(\mathcal{A}_1) = s(\mathcal{A}_2) = 136$ precisely. The radar plot can be seen in figure 3.9(a).

Next the control parameter $\alpha = 1$ is set. It leads to the emergence of a standard basin boundary of the NDDS. Simulations reveal that the likelihood of outcomes is almost even now: $s(\mathcal{A}_3) = 259$ cases go to the attractor $\mathcal{A}_3$ while 268 cases are attracted by $\mathcal{A}_1$ and $\mathcal{A}_2$ each. The result is shown in figure 3.9(b).

Finally, the control parameter $\alpha = 1 + 0.005i$ is chosen. It leads to the emergence of a rotated boundary. After inspecting the outcomes, the change in situation is seen: attractor $\mathcal{A}_2$ is now dominant with $s(\mathcal{A}_2) = 472$ cases while $\mathcal{A}_1$ and $\mathcal{A}_3$ attract 261 and 62 different initial seeds respectively. The visual outcome is shown in figure 3.9(c).

α	$s(\mathcal{A}_1)$	$s(\mathcal{A}_2)$	$s(\mathcal{A}_3)$
0.97	136	136	523
1	268	268	259
$1 + 0.005i$	261	472	62

Table 3.1: Distribution of simulations (out of $s = 795$) that go to different attractors $\mathcal{A}_1$, $\mathcal{A}_2$, $\mathcal{A}_3$ under various values of parameter α.

The overall resulting situation is reviewed in table 3.1 and presented visually in figure 3.9.

To sum up, some complicated interactions between the resulting attractors are observed during simulations. Moreover, these interactions involve more than two attractors simultaneously. This means that during research it is crucial to consider not only the boundary itself (in terms of fractal dimension or equivalent characteristic) but also the neighboring basins of attraction (in terms of Wada measure or some other means).

3.2.2. Controlling the dynamical system

In some cases it is important to stabilize and control the nonlinear dynamical system as required. It is not always an easy task. Some particular initial seeds are chosen $z_0 \in \{-0.793 - 0.001i, -0.793, -0.793 + 0.001i\}$, then the evolution of dynamics is observed while the control parameter $\alpha = 1$ is slightly perturbed until $\alpha = 0.99$.

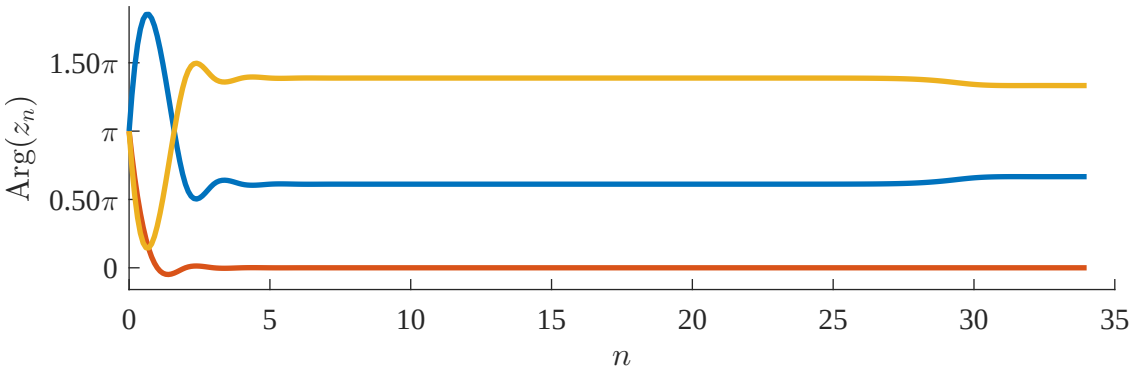

(a) $\alpha = 1$;

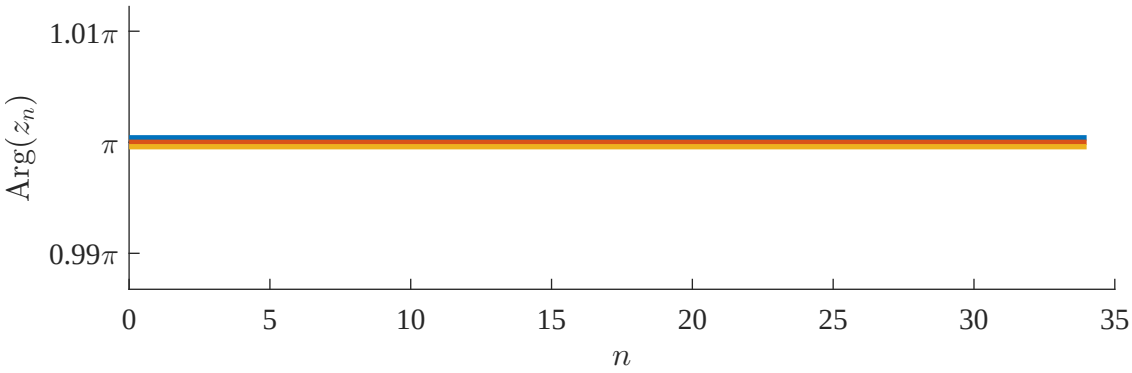

(b) $\alpha = 0.99$.

Figure 3.10: Trajectories of the Nn orbits when the initial seed $z_0 = -0.793$ varies by $\Delta z = 0.001i$ and the parameter α is slightly perturbed.

It is not possible to plot complex orbits in less than three dimensions so other acceptable ways of representing the situation are considered. Because of fluctuations in magnitude that occur while observing orbits the complex arguments (see figure 3.10) are plotted. Understandably the convergence of arguments does not ensure the convergence of values hence this aspect is checked separately.

Then $\alpha = 1$ is set along with aforementioned initial seeds which have the property $\mathrm{Arg}(z_0) \approx \pi$. As the orbits evolve the trajectories diverge briefly, approximately until iteration $n = 4$ and begin to stabilize afterwards. By the time the iteration $n = 35$ is reached, the arguments are stable and

so are the values. In fact the values have converged to three distinct attractors $\mathcal{A}_1,\ \mathcal{A}_2,\ \mathcal{A}_3$. The values are shown in figure 3.10(a).

In another case the control parameter is perturbed to $\alpha = 0.99$. It is a relatively slight shift yet the effect is critical. All initial seeds remain the same and the property $\mathrm{Arg}(z_0) \approx \pi$ does not change during iterations. In fact the values continue to remain in the starting region during the whole experimental period $n = \overline{0, \ldots, 35}$. These orbits are presented in figure 3.10(b).

To sum up the trajectories of orbits depend on the control parameter α. In case of more than two attractors the final outcomes are attracted by multiple distinct regions. Therefore, the ability to predict convergence of an arbitrary initial seed is influenced not only by the positioning and complexity of the basin boundary but also by the intertwining of the basins themselves. While the formal aspect can be somewhat measured using fractal dimension, the latter requires Wada measure or equivalent tools.

3.3. Discussion

Newton's discrete dynamical system is analyzed numerically in terms of basins of attraction $\mathcal{B}$ and their fractal boundaries $\partial\mathcal{B} = \mathcal{F}$, using control parameter $\alpha \in \mathbb{C}$.

Fractal dimension D is evaluated using the box counting technique. Some peculiar dynamical processes are noticed, especially when the imaginary part of α varies, revealing periodic-like behavior. The dimension itself fluctuates from $D = 1$ in a trivial case, to $D = 1.68$ for a very complicated structure.

Wada measure W is calculated using a novel proposed algorithm. The results only somewhat resemble those concerning fractal dimension. Most notably the proposed Wada characteristic also takes into account the basins of attraction. The measure itself varies from $W = 0.03$ in a trivial case, to $W = 0.99$ for especially intertwined boundaries.

The relation between characteristics D and W is highly non-trivial. There is a positive correlation but nothing like a bijective correspondence can be defined. This is understandable since Wada measure takes into account more data.

The uncertainty of the final attractor $\mathcal{A}$ is examined. It can be an extremely complicated task to determine when (and where) a specific trajectory converges. This difficulty to predict the outcome can be evaluated quantitatively in terms of both characteristics.

Unlike other research, the limited precision is emphasized in this work. It means that once the grid of value simulations is obtained, it is not possible to zoom in order to obtain an even more detailed picture of the model. This apparent drawback can also be seen as a realistic situation when only some experimental observations are available instead of the precise model.

Conclusions

1. Relaxed Newton's discrete dynamical system exhibits rich dynamics and a high variety of set-ups of attracting basins, using parameters $\alpha \in \mathbb{C}_1$ and $p(z) = z^3 - 1$.

2. Fractal dimension is found to be in range $D(\mathcal{F}_\alpha) \in [1, 1.68]$ when $\alpha \in \mathbb{C}_1$. However, it can be higher when $\alpha \in \mathbb{C}$.

3. Wada measure is found to be in range $W(\mathcal{F}_\alpha) \in [0.03, 0.99]$ when $\alpha \in \mathbb{C}_1$.

4. There exists a non-trivial relation between $D(\mathcal{F})$ and $W(\mathcal{F})$.
   Pearson's correlation coefficient $\rho = 0.82$.
   Spearman's correlation coefficient $r = 0.87$.

5. Slight perturbations to the control parameter α may cause extreme changes in the long-term behavior of trajectories.

6. In order to better characterize a dynamical system, Wada measure W should be used in pair with fractal dimension D.

Bibliography

[1] S. Strogatz, *Nonlinear Dynamics and Chaos: An Introduction*. Westview Press, 2014.

[2] J. Hubbard, D. Schleicher, and S. Sutherland, "How to find all roots of complex polynomials by Newton's method," *Inventiones Mathematicae*, vol. 146, no. 1, pp. 1–33, 2001.

[3] I. J. Sobey, *Characteristics of Newton's Method on Polynomials*. Oxford Computer Lab, 1996.

[4] B. Epureanu and H. Greenside, "Basins of attraction associated with a Newton's method," *SIAM review*, vol. 40, no. 1, pp. 102–199, 1998.

[5] D. M. Burton, *The History of Mathematics: An Introduction*. McGraw-Hill, 2007.

[6] C. B. Boyer, *A History of Mathematics*. Wiley, 1991.

[7] P. J. Nahin, *An Imaginary Tale: The Story of "i" [the square root of minus one]*. Princeton University Press, 2010.

[8] A. Friedman, *Foundations of Modern Analysis*. Courier Corporation, 1970.

[9] Hans Lundmark and H. Lundmark, *Visualizing complex analytic functions using domain coloring*. Linköping University, 2004.

[10] A. Terentiev, V. Zhitnikov, and N. Dimitrieva, "An application of analytic functions to axisymmetric flow problems," *Applied Mathematical Modelling*, vol. 21, pp. 91–96, feb 1997.

[11] L. M. Milne-Thomson, *Theoretical Aerodynamics*. Courier Corporation, 2012.

[12] A. Oz and S. Hershkovitz, "Analysis of impedance spectroscopy of aqueous supercapacitors by evolutionary programming," *Solid State Ionics*, nov 2015.

[13] E. Nelson, "Derivation of the Schrödinger Equation from Newtonian Mechanics," *Physical Review*, vol. 150, pp. 1079–1085, oct 1966.

[14] H. K. Khalil, *Nonlinear Systems*. Prentice Hall, 2002.

[15] J. M. T. Thompson and H. B. Stewart, *Nonlinear Dynamics and Chaos*. John Wiley & Sons, 2002.

[16] A. Katok and B. Hasselblatt, *Introduction to the Modern Theory of Dynamical Systems*. Cambridge University Press, 1997.

[17] O. Galor, *Discrete Dynamical Systems*. Springer, 2007.

[18] R. L. Devaney, *An Introduction to Chaotic Dynamical Systems*. Westview Press, 2003.

[19] R. C. Hilborn, *Chaos and Nonlinear Dynamics: An Introduction for Scientists and Engineers*. Oxford University Press, 2000.

[20] L. Arnold and V. Wihstutz, eds., *Lyapunov Exponents*, vol. 1186 of *Lecture Notes in Mathematics*. Springer Berlin Heidelberg, 1986.

[21] T. Riedrich, *An Introduction to Hankel Operators.*, vol. 71. Cambridge University Press, 1991.

[22] T. Muir and W. Metzler, *A Treatise on the Theory of Determinants*. Courier Corporation, 2003.

[23] M. Landauskas and M. Ragulskis, "A pseudo-stable structure in a completely invertible bouncer system," *Nonlinear Dynamics*, vol. 78, pp. 1629–1643, jul 2014.

[24] F. Li, H. A. Wantuch, R. J. Linger, E. J. Belikoff, and M. J. Scott, "Transgenic sexing system for genetic control of the Australian sheep blow fly Lucilia cuprina.," *Insect biochemistry and molecular biology*, vol. 51, pp. 80–8, aug 2014.

[25] L. Lanfumey, R. Mongeau, and M. Hamon, "Biological rhythms and melatonin in mood disorders and their treatments.," *Pharmacology & therapeutics*, vol. 138, pp. 176–84, may 2013.

[26] S. Dinicola, F. D'Anselmi, A. Pasqualato, S. Proietti, E. Lisi, A. Cucina, and M. Bizzarri, "A systems biology approach to cancer: fractals, attractors, and nonlinear dynamics.," *Omics : a journal of integrative biology*, vol. 15, pp. 93–104, mar 2011.

[27] G. Dwyer, J. Dushoff, and S. Yee, "The combined effects of pathogens and predators on insect outbreaks," *Nature*, 2004.

[28] B. K. Williams, J. D. Nichols, and M. J. Conroy, *Analysis and Management of Animal Populations*. Academic Press, 2001.

[29] A. A. Houck, H. E. Türeci, and J. Koch, "On-chip quantum simulation with superconducting circuits," *Nature Physics*, vol. 8, pp. 292–299, apr 2012.

[30] P. Tassin, L. Zhang, R. Zhao, A. Jain, T. Koschny, and C. M. Soukoulis, "Electromagnetically induced transparency and absorption in metamaterials: the radiating two-oscillator model and its experimental confirmation.," *Physical review letters*, vol. 109, p. 187401, nov 2012.

[31] P. Gatti, *Applied Structural and Mechanical Vibrations: Theory and Methods*. CRC Press, 2014.

[32] C. Wu and S. Gharavi, *Radar Conference (EuRAD), 2013 European*. EuRAD, 2013.

[33] A. H. Gandomi, X.-S. Yang, and A. H. Alavi, “Cuckoo search algorithm: a metaheuristic approach to solve structural optimization problems,” *Engineering with Computers*, vol. 29, pp. 17–35, jul 2011.

[34] G. Madjarov, D. Kocev, D. Gjorgjevikj, and S. Džeroski, “An extensive experimental comparison of methods for multi-label learning,” *Pattern Recognition*, vol. 45, pp. 3084–3104, sep 2012.

[35] M. Yamuna and A. Das, “Multiple Message Encryption using Euler Graphs,” *International Journal of Computer Science*, 2014.

[36] A. Bunde and S. Havlin, *Fractals in Science*. Springer, 1994.

[37] B. B. Mandelbrot, *The Fractal Geometry of Nature*. Einaudi paperbacks, Henry Holt and Company, 1983.

[38] T. Martyn, “A new approach to morphing 2D affine IFS fractals,” *Computers and Graphics (Pergamon)*, vol. 28, pp. 249–272, apr 2004.

[39] G. Helmberg, *Getting Acquainted with Fractals*. Walter de Gruyter, 2007.

[40] S. Jampala, “Fractals: classification, generation and applications,” in *Proceedings of the 35th Midwest Symposium on Circuits and Systems*, pp. 1024–1027, IEEE, 1992.

[41] A. F. Beardon, *Iteration of Rational Functions: Complex Analytic Dynamical Systems*. Springer Science & Business Media, 2000.

[42] K. Falconer, *Fractal Geometry: Mathematical Foundations and Applications*. Wiley, 2007.

[43] M. F. Barnsley and H. Rising, *Fractals Everywhere*. Morgan Kaufmann, 2000.

[44] D. H. Hepting and J. C. Hart, “The Escape Buffer: Efficient Computation of Escape Time for Linear Fractals,” *Graphics Interface ’95*, pp. 204–214, 1995.

[45] B. J. Cole, “Fractal time in animal behaviour: the movement activity of Drosophila,” *Animal Behaviour*, vol. 50, no. 5, pp. 1317–1324, 1995.

[46] V. O. Nams and M. Bourgeois, “Fractal analysis measures habitat use at different spatial scales: an example with American marten,” *Canadian Journal of Zoology*, vol. 82, pp. 1738–1747, nov 2004.

[47] L. A. Mirny, “The fractal globule as a model of chromatin architecture in the cell.,” *Chromosome research*, vol. 19, pp. 37–51, jan 2011.

[48] R. Voss, “Evolution of long-range fractal correlations and 1/f noise in DNA base sequences.,” *Physical review letters*, vol. 68, pp. 3805–3808, jun 1992.

[49] B. G. Elmegreen, “A Fractal Origin for the Mass Spectrum of Interstellar Clouds,” *The Astrophysical Journal*, vol. 564, pp. 773–781, jan 2002.

[50] G. Iovane, E. Laserra, and F. Tortoriello, “Stochastic self-similar and fractal universe,” *Chaos, Solitons & Fractals*, vol. 20, pp. 415–426, may 2004.

[51] F. Labini, A. Gabrielli, M. Montuori, and L. Pietronero, “Finite size effects on the galaxy number counts: Evidence for fractal behavior up to the deepest scale,” *Physica A: Statistical Mechanics and its Applications*, vol. 226, pp. 195–242, may 1996.

[52] C. Puente-Baliarda, J. Romeu, R. Pous, and A. Cardama, “On the behavior of the Sierpinski multiband fractal antenna,” *IEEE Transactions on Antennas and Propagation*, vol. 46, pp. 517–524, apr 1998.

[53] M. S. Taqqu, V. Teverovsky, and W. Willinger, “Is Network Traffic Self-Similar or Multifractal?,” *Fractals*, vol. 05, pp. 63–73, mar 1997.

[54] M. Batty and P. Longley, “Urban shapes as fractals,” *Area*, 1987.

[55] Y. Fisher, “Fractal Image Compression,” *Fractals*, vol. 02, pp. 347–361, sep 1994.

[56] H. Lantuit and V. Rachold, “Towards a calculation of organic carbon release from erosion of Arctic coasts using non-fractal coastline datasets,” *Marine Geology*, vol. 257, pp. 1–10, feb 2009.

[57] R. Taylor, “Reduction of Physiological Stress Using Fractal Art and Architecture,” *Leonardo*, vol. 39, pp. 245–251, jun 2006.

[58] K. E. Atkinson, *An Introduction to Numerical Analysis*. Wiley, 1978.

[59] E. Schröder, “Ueber unendlich viele Algorithmen zur Auflösung der Gleichungen,” *Mathematische Annalen*, vol. 2, pp. 317–365, jun 1870.

[60] A. Cayley, “Application of the Newton-Fourier method to an imaginary root of an equation,” *Quart. J. Pure Appl. Math*, 1879.

[61] M. Drexler, I. Sobey, and C. Bracher, *Fractal Characteristics of Newton’s Method on Polynomials*. Oxford University Computer Laboratory, 1996.

[62] P. Fatou, “Sur les équations fonctionnelles,” *Bulletin de la Société mathématique de France*, 1919.

[63] G. Julia, “Mémoire sur l’iteration des fonctions rationnelles,” *Journal de Mathématiques Pures et Appliquées*, vol. 8, pp. 47–245, 1918.

[64] R. Holt and I. Schwartz, “Newton’s method as a dynamical system: Global convergence and predictability,” *Physics Letters A*, vol. 105, pp. 327–333, oct 1984.

[65] W. J. Gilbert, “Generalizations of Newton’S Method,” *Fractals*, vol. 09, pp. 251–262, sep 2001.

[66] H. Susanto and N. Karjanto, “Newton’s method’s basins of attraction revisited,” *Applied Mathematics and Computation*, vol. 215, pp. 1084–1090, oct 2009.

[67] J. Walsh, “The dynamics of Newton’s method for cubic polynomials,” *The College Mathematics Journal*, 1995.

[68] P. S. Jr, “Newton’s method and fractal patterns,” *Applications of Calculus*, 1991.

[69] J. H. Cartwright, “Newton maps: fractals from Newton’s method for the circle map,” *Computers & Graphics*, vol. 23, pp. 607–612, aug 1999.

[70] M. Drexler, I. Sobey, and C. Bracher, *On the fractal characteristics of a stabilised Newton method*. Oxford University Computing Laboratory, 1995.

[71] D. Chandra Sekhar and R. Ganguli, “Fractal boundaries of basin of attraction of Newton–Raphson method in helicopter trim,” *Computers & Mathematics with Applications*, vol. 60, pp. 2834–2858, nov 2010.

[72] B. I. Epureanu and H. S. Greenside, “Fractal Basins of Attraction Associated with a Damped Newton’s Method,” *SIAM Review*, vol. 40, pp. 102–109, jan 1998.

[73] M. Frame and N. Neger, “Newton’s Method and the Wada Property: A Graphical Approach,” *The College Mathematics Journal*, vol. 38, pp. 192–204, apr 2007.

[74] M. Amrein and T. P. Wihler, “An adaptive Newton-method based on a dynamical systems approach,” *Communications in Nonlinear Science and Numerical Simulation*, vol. 19, pp. 2958–2973, sep 2014.

[75] X. Wang and X. Yu, “Julia sets for the standard Newton’s method, Halley’s method, and Schröder’s method,” *Applied Mathematics and Computation*, vol. 189, pp. 1186–1195, jun 2007.

[76] J. M. Lee, *Introduction to Topological Manifolds*. Springer Science & Business Media, 2000.

[77] E. F. Krause, *Taxicab Geometry: An Adventure in Non-Euclidean Geometry*. Courier Corporation, 1975.

[78] F. Caserta and W. Eldred, “Determination of fractal dimension of physiologically characterized neurons in two and three dimensions,” *Journal of Neuroscience Methods*, vol. 56, pp. 133–144, feb 1995.

[79] C. Fortin, R. Kumaresan, W. Ohley, and S. Hoefer, “Fractal dimension in the analysis of medical images,” *IEEE Engineering in Medicine and Biology Magazine*, vol. 11, pp. 65–71, jun 1992.

[80] B. Chaudhuri and N. Sarkar, "Texture segmentation using fractal dimension," *IEEE Transactions on Pattern Analysis and Machine Intelligence*, vol. 17, no. 1, pp. 72–77, 1995.

[81] J. Kennedy and J. A. Yorke, "Basins of Wada," *Physica D: Nonlinear Phenomena*, vol. 51, pp. 213–225, aug 1991.

[82] H. E. Nusse and J. A. Yorke, "Wada basin boundaries and basin cells," *Physica D: Nonlinear Phenomena*, vol. 90, pp. 242–261, feb 1996.

[83] Y. Zhang and G. Luo, "Unpredictability of the Wada property in the parameter plane," *Physics Letters A*, vol. 376, pp. 3060–3066, oct 2012.

[84] R. Breban and H. E. Nusse, "On the creation of Wada basins in interval maps through fixed point tangent bifurcation," *Physica D: Nonlinear Phenomena*, vol. 207, pp. 52–63, jul 2005.

[85] J. Aguirre and M. A. Sanjuán, "Unpredictable behavior in the Duffing oscillator: Wada basins," *Physica D: Nonlinear Phenomena*, vol. 171, pp. 41–51, oct 2002.

[86] L. Poon, J. Campos, O. Edward, and C. Grebogi, "Wada Basin Boundaries in Chaotic Scattering," *International Journal of Bifurcation and Chaos*, vol. 06, pp. 251–265, feb 1996.

[87] D. Sweet, E. Ott, and J. A. Yorke, "Topology in chaotic scattering," *Nature*, vol. 399, pp. 315–316, may 1999.

[88] S. Portela and E. Iber, "Fractal and Wada Exit Basin Boundaries in Tokamaks," *International Journal of Bifurcation and Chaos*, vol. 17, pp. 4067–4079, nov 2007.

[89] J. Vandermeer, "Wada basins and qualitative unpredictability in ecological models: a graphical interpretation," *Ecological Modelling*, vol. 176, pp. 65–74, aug 2004.

[90] J. Vandermeer, L. Stone, and B. Blasius, "Categories of chaos and fractal basin boundaries in forced predator–prey models," *Chaos, Solitons & Fractals*, vol. 12, pp. 265–276, jan 2001.

[91] Y. Zhang and G. Luo, "Wada bifurcations and partially Wada basin boundaries in a two-dimensional cubic map," *Physics Letters A*, vol. 377, pp. 1274–1281, aug 2013.

[92] A. Daza, A. Wagemakers, M. A. F. Sanjuán, and J. A. Yorke, "Testing for Basins of Wada.," *Scientific reports*, vol. 5, p. 16579, jan 2015.

[93] E. Ott, *Chaos in Dynamical Systems*. Cambridge University Press, 2002.